

# **Regulation of chloroplast NADH dehydrogenase-like complex by NADPH-dependent thioredoxin system**

Short title: NTRC regulates the thylakoid NDH complex

Lauri Nikkanen, Jouni Toivola, Andrea Trotta, Manuel Guinea Diaz, Mikko Tikkanen, Eva-Mari Aro  
and Eevi Rintamäki

Molecular Plant Biology, Department of Biochemistry, University of Turku, FI-20014 Turku, Finland

Corresponding author:

Eevi Rintamäki

[evirin@utu.fi](mailto:evirin@utu.fi)

Molecular Plant Biology

University of Turku

FI-20014 TURKU

Finland

+358504309491

The author responsible for distribution of materials integral to the findings presented in this article in accordance with the policy described in the Instructions for Authors ([www.plantcell.org](http://www.plantcell.org)) is: Eevi Rintamäki ([evirin@utu.fi](mailto:evirin@utu.fi)).

## ABSTRACT

Linear electron transport in the thylakoid membrane drives both photosynthetic NADPH and ATP production, while cyclic electron flow (CEF) around photosystem I only promotes the translocation of protons from stroma to thylakoid lumen. The chloroplast NADH-dehydrogenase-like complex (NDH) participates in one CEF route transferring electrons from ferredoxin back to the plastoquinone pool with concomitant proton pumping to the lumen. CEF has been proposed to balance the ratio of ATP/NADPH production and to control the redox poise particularly in fluctuating light conditions, but the mechanisms regulating the NDH complex remain unknown. We have investigated the regulation of the CEF pathways by the chloroplast NADPH-thioredoxin reductase (NTRC) *in vivo* by using an Arabidopsis knockout line of *NTRC* as well as lines overexpressing NTRC. Here we present biochemical and biophysical evidence showing that NTRC activates the NDH-dependent CEF and regulates the generation of proton motive force, thylakoid conductivity to protons and redox homeostasis between the thylakoid electron transfer chain and the stroma during changes in light conditions. Further, protein-protein interaction assays suggest a putative TRX-target site in close proximity to the ferredoxin binding domain of NDH, thus providing a plausible mechanism for regulation of the NDH ferredoxin:plastoquinone oxidoreductase activity by NTRC.

# INTRODUCTION

In their natural habitats, plants face constant fluctuation of light intensity, including both seasonal changes in photoperiod and daily fluctuations according to environmental conditions. Optimization of photosynthesis in plant leaves requires strict balancing between conversion of light energy to chemical energy in photosynthetic light reactions and the energy-consuming reactions of chloroplast metabolism. Multiple regulatory and photoprotective mechanisms have evolved in photosynthetic organisms to cope with fluctuating light conditions and to prevent the photodamage of both Photosystem (PS) II and PSI (Tikkanen et al., 2012; Tikkanen and Aro, 2014; Tiwari et al., 2016; Townsend et al., 2017). Regularly occurring light variations induce long-term acclimatory changes in the photosynthetic machinery via signaling mechanisms, while temporary fluctuation of light within a day transiently activates short-term regulatory mechanisms (Bailey et al., 2001; Grieco et al., 2012; Kono and Terashima, 2014; Armbruster et al., 2014). The short-term mechanisms include non-photochemical quenching (NPQ), photosynthetic control of electron flow between PSII and PSI, state transitions (ST), cyclic electron flow (CEF), and activation of photosynthetic enzymes both in light and carbon fixation reactions (Demmig-Adams et al., 2012; Tikkanen and Aro, 2014; Balsera et al., 2014; Yamori et al., 2016; Gollan et al., 2017). Discovery of redox-regulated activation of Calvin Benson Cycle (CBC) enzymes by chloroplast thioredoxins was the first indication of direct regulatory coupling between photosynthetic light reactions and carbon fixation reactions (reviewed by (Buchanan, 2016). Later on, thioredoxins have been shown to be involved also in the regulation of thylakoid electron flow via redox-control of the ATP synthase (McKinney et al., 1978; Nalin and McCarty, 1984), the STN7 kinase (Rintamäki et al., 2000), and NPQ (Hall et al., 2010; Brooks et al., 2013; Hallin et al., 2015; Naranjo et al., 2016), suggesting that thioredoxins are important members of the chloroplast regulatory network controlling photosynthetic redox balance in fluctuating light conditions (Nikkanen and Rintamäki, 2014).

Light drives the electron flow from water through PSII, plastoquinone (PQ), cytochrome *b6f*, plastocyanin (PC) and PSI to ferredoxin and ultimately to NADP<sup>+</sup>, producing NADPH. These photosynthetic electron transfer reactions are coupled to ATP synthesis via translocation of protons to the thylakoid lumen, generating a proton gradient over the thylakoid membrane ( $\Delta pH$ ), which together with membrane potential ( $\Delta \Psi$ ) constitutes the proton motive force (*pmf*) (Junesch and Gräber, 1991; Armbruster et al., 2017).  $\Delta pH$  also contributes to induction of NPQ, a photoprotective mechanism that

88 dissipates excess excitation energy from the electron transfer chain (Niyogi and Truong, 2013; Ruban,  
89 2016), and maintains photosynthetic control at Cyt *b6f* (Joliot and Johnson, 2011; Johnson, 2011).  
90 Other regulatory mechanisms include the reversible rearrangements of light harvesting complexes to  
91 balance the excitation of PSII and PSI known as state transitions (Tikkanen et al., 2006; Ruban and  
92 Johnson, 2009; Rochaix, 2011) as well as cyclic electron flow around PSI (CEF), a process where  
93 electrons are transferred from ferredoxin back to the PQ pool. CEF contributes to generation of  $\Delta pH$   
94 and therefore to production of ATP, and has been suggested to adjust the ATP/NADPH ratio in  
95 chloroplasts according to the needs of the CBC (for a recent review, see (Yamori and Shikanai, 2016)).  
96 Moreover, CEF provides an alternative electron valve to relieve stromal over-reduction that is needed  
97 to protect the photosystems from damage during early developmental stages of chloroplasts (Allorent et  
98 al., 2015; Suorsa, 2015) and during excess illumination or fluctuating light conditions (Miyake et al.,  
99 2004; Suorsa et al., 2012; Yamori and Shikanai, 2016; Yamori et al., 2016). CEF has also been shown  
100 to be important for regulation of the proton motive force (Wang et al., 2015; Shikanai and Yamamoto,  
101 2017), and during induction of photosynthesis (Joliot and Joliot, 2002; Fan et al., 2007). Fan et al.  
102 (2007) calculated that CEF contributes a maximum of 68% of total electron flux after 30 s illumination  
103 of spinach leaves with red and far red light.

104 Two distinct and partially redundant pathways of CEF have been suggested to exist in plant  
105 chloroplasts (Munekage et al., 2004). One CEF pathway involves the chloroplast NADH  
106 dehydrogenase-like complex (NDH), an orthologue of mitochondrial respiratory complex I (Shikanai,  
107 2016; Peltier et al., 2016). However, unlike complex I, which is reduced by NADH, the chloroplast  
108 NDH complex is reduced by ferredoxin (Yamamoto et al., 2011; Yamamoto and Shikanai, 2013). It has  
109 been suggested recently in several studies that CEF via the NDH complex is essential for  
110 photosynthesis in low light conditions (Yamori et al., 2015; Kou et al., 2015; Martin et al., 2015) as  
111 well as for the tolerance of drought (Horvath et al., 2000) and low temperature (Yamori et al., 2011).  
112 The antimycin A –sensitive CEF pathway depends on the proteins PROTON GRADIENT  
113 REGULATION 5 (PGR5) (Munekage et al., 2002) and PGR5-LIKE 1 (PGRL1) (DalCorso et al.,  
114 2008), and has been suggested to constitute the hypothetical ferredoxin-plastoquinone reductase (FQR)  
115 (Hertle et al., 2013). However, controversy still exists over the molecular identity of FQR and the  
116 physiological function of PGR5 (Leister and Shikanai, 2013; Tikkanen and Aro, 2014; Kanazawa et al.  
117 2017). In general, the CEF activity is highly dependent on stromal redox state (Breyton et al., 2006). In

fact, both the PGR-dependent pathway (Hertle et al., 2013; Strand et al., 2016a) and the NDH pathway (Courteille et al., 2013) have been proposed to be subject to thiol-regulation by stromal thioredoxins.

In chloroplasts of higher plants, two thioredoxin systems function in parallel. The Ferredoxin-thioredoxin system depends on photosynthetically reduced ferredoxin to supply electrons to the Ferredoxin-thioredoxin reductase (FTR), which in turn reduces several thioredoxins, namely TRX-*f1* and *f2*, four isoforms of TRX-*m*, TRX-*x* as well as TRX-*y1* and *y2* (Schürmann and Buchanan, 2008; Yoshida and Hisabori, 2017). The other system consists of a single enzyme, NADPH-thioredoxin reductase (NTRC) that contains both a reductase and a thioredoxin domain (Serrato et al., 2004). NTRC is reduced by NADPH, which is produced, besides in the light reactions, also in the oxidative pentose phosphate pathway (OPPP) in darkness. Both chloroplast TRX systems are essential for normal development and growth of plants (Serrato et al., 2004; Wang et al., 2014). The *ntrc* knockout has a stunted and low chlorophyll phenotype, which is particularly severe in plants grown under short photoperiods (Perez-Ruiz et al., 2006; Lepistö et al., 2009; Lepistö et al., 2013). The mutant suffers from impaired ability to activate the ATP synthase and CBC enzymes as well as elevated non-photochemical quenching (NPQ) (Nikkanen et al., 2016; Carrillo et al., 2016; Naranjo et al., 2016; Thormählen et al., 2017). In contrast, the NTRC overexpression line (OE-NTRC), with 15–20 times higher NTRC content compared to WT, shows enhanced vegetative growth and increased activation of the ATP synthase and CBC enzymes particularly in darkness and low light (Toivola et al., 2013; Nikkanen et al., 2016). NTRC has a less negative midpoint redox potential than FTR (Hirasawa et al., 1999; Yoshida and Hisabori, 2016) and plays an important regulatory role under low irradiance, while the FTR-dependent system probably requires more extensive illumination to be fully activated (Thormählen et al., 2017; Geigenberger et al., 2017; Nikkanen et al., 2016). Recent studies have revealed significant functional overlap and crosstalk between the two chloroplast TRX systems, and indicated that they cooperatively regulate ATP synthesis, the CBC, starch synthesis and scavenging of reactive oxygen species (ROS) (Thormählen et al., 2015; Nikkanen et al., 2016; Pérez-Ruiz et al., 2017; Geigenberger et al., 2017). Moreover, redox-regulation of both CEF pathways has been previously reported (Courteille et al., 2013; Hertle et al., 2013; Strand et al., 2016a). The physiological roles of each CEF pathway and TRXs involved in the regulation are nevertheless still unclear.

Here we have used the *ntrc* knockout mutant as well as NTRC overexpression lines of *Arabidopsis thaliana* to investigate the potential role of the NTRC system in regulating CEF. Our results emphasize

the important role of thioredoxins in the chloroplast regulatory network, particularly controlling the photosynthetic redox balance under fluctuating light conditions. NTRC plays a crucial role in activation of the NDH-dependent CEF in darkness (chlororespiration) and during dark to light transitions. Overexpression of NTRC, on the other hand, maintains constant NDH-CEF activity leading to elevated *pmf* and improved utilization of light energy under fluctuating light conditions. Our results also suggest that NTRC does not activate the PGR-dependent CEF, but contributes to the PGR5-dependent downregulation of thylakoid membrane proton conductivity upon transitions to high light intensity. Through control of both CEF and the activity of the ATP synthase, NTRC plays a pivotal role in adjusting the proton motive force and photosynthetic redox poise in Arabidopsis chloroplasts.

## RESULTS

### NTRC is an active reductant in dark and in low light conditions

NADPH produced in the oxidative pentose phosphate pathway (OPPP) has been proposed to maintain NTRC partially reduced, and thus active in darkness and when low irradiance limits photosynthesis (Perez-Ruiz et al., 2006; Geigenberger et al., 2017). To confirm this hypothesis, we analyzed the *in vivo* redox state of NTRC by a mobility shift assay using the WT or OE-NTRC protein extracts alkylated with methoxypolyethylene glycol maleimide (MAL-PEG). The assays indicated that NTRC redox state remains fairly constant in all light intensities and during dark-to-light transitions, with a significant proportion of the enzyme pool in fully or partially reduced form (Fig. 1A and 1C). This is also the case in OE-NTRC, despite the increase in NTRC content of leaves (Fig. 1B, Suppl. Fig. 1A). These results are in agreement with the hypothesis that NTRC acts as a thiol regulator of photosynthesis and chloroplast metabolism in darkness and low light conditions (Nikkanen et al., 2016; Carrillo et al., 2016; Thormählen et al., 2017).

### NDH-dependent CEF is enhanced by overexpression of NTRC

In order to determine the effect of altered chloroplast thiol-redox state on the activity of NDH-dependent CEF, we measured the post-illumination rise of chlorophyll a fluorescence (PIFR). The PIFR has been suggested to represent electron flow from stromal reductants via the NDH-complex to

the plastoquinone (PQ) pool upon cessation of illumination (Shikanai et al., 1998; Gotoh et al., 2010). The OE-NTRC line showed a significantly larger PIFR after pre-illumination with low intensity white light than WT, suggesting increased CEF activity (Fig. 2A). In agreement with previous reports, no PIFR was detected in the *ndho* mutant, which is lacking a functional NDH complex (Rumeau et al., 2005), while a diminished PIFR was observed in the *pgr5* line, which is deficient in PGR-dependent CEF (Munekage et al., 2002) (Fig. 2B). These results suggest that NTRC contributes to activation of NDH-dependent CEF. In order to confirm that the increased PIFR in OE-NTRC derives from the activity of the NDH complex, we generated an NTRC overexpression line in the *ndho* mutant background (OE-NTRC *ndho*). PIFR was indeed fully eliminated in that line (Fig. 2C). The level of NTRC overexpression in OE-NTRC *ndho* plants was confirmed by immunoblotting and found to be similar to the OE-NTRC line (Suppl. Fig. 1B).

The *ntrc* knockout exhibited a slower initial PIFR response after 500 s of light, but the PIFR did not decline after 15–20 s as in WT or OE-NTRC, but instead continued to rise throughout the duration of the dark phase of the experiment (Fig. 2A). A brief pulse of far red (FR) light quenched the fluorescence, but after cessation of the FR light, fluorescence quickly rose back to its high pre-FR level. The  $F_0$  level was elevated in dark-adapted *ntrc* leaves compared to WT, OE-NTRC or other mutant lines (Fig. 2A). The abnormal fluorescence pattern in Fig. 2A may also be due to the highly pleiotropic phenotype of the *ntrc* mutant, particularly when grown under a short day photoperiod. To clarify whether the differences in PIFR were caused indirectly by metabolic disturbances due to impaired growth in a short photoperiod, we repeated the experiment with plants grown in a 12h/12h photoperiod. PIFR mostly disappeared in 12h photoperiod grown *ntrc*, but remained similar to 8h photoperiod grown plants in WT and OE-NTRC (Suppl. Fig. 2A).

## **NTRC increases dark-reduction of the plastoquinone pool**

As overexpression of NTRC increased NDH-dependent CEF in darkness after illumination (Fig. 2), we analyzed the phosphorylation level of LHCII proteins in dark-adapted and illuminated leaves to determine if the higher CEF activity alters the redox state of the PQ pool. Reduction of the PQ pool induces phosphorylation of LHCII by activating the STN7 kinase through interaction with the Cyt *b6f* complex (Vener et al., 1997; Bellafiore et al., 2005; Shapiguzov et al., 2016). In WT LHCII proteins

were mostly non-phosphorylated in darkness, maximally phosphorylated in low light, moderately phosphorylated in growth light and mostly de-phosphorylated in high light (Fig. 3H), in agreement with earlier studies (Rintamäki et al., 1997; Tikkanen et al., 2010). The *stn7* mutant was unable to phosphorylate LHCII (Bellafigliore et al., 2005). In contrast to WT, LHCII was phosphorylated in darkness in OE-NTRC (Fig. 3H). As in WT, only a small amount of phosphorylated LHCII was present in thylakoids isolated from dark-adapted leaves of *ntrc*. Interestingly, de-phosphorylation of LHCII proteins in high light was slightly impaired in *ntrc* (Fig. 3A). This is in accordance with earlier studies showing that phosphorylation of LHCII is highly dependent on stromal thiol redox state in high light (Rintamäki et al., 2000; Martinsuo et al., 2003).

To further investigate the effect of NTRC on PQ pool reduction in darkness, we measured the kinetics of Chl a fluorescence OJIP transients in dark-adapted leaves and in leaves pre-illuminated with far red light (FR) to fully oxidize the PQ pool. The difference in  $F/F_m$  at the J phase of the transient ( $F_J$ , 3 ms after onset of illumination) between dark-adapted and pre-illuminated leaves is an indicator for the redox state of the PQ pool in darkness (Toth et al., 2007; Stirbet et al., 2014). The results suggested a significantly larger proportion of reduced PQ in darkness in the OE-NTRC line when compared to WT (Fig. 3A–B, Suppl. Table S1). The *ndho* mutant had a more oxidized PQ pool in darkness than WT, while there was no significant difference between *pgr5* and WT (Fig. 3G), suggesting that the NDH complex is the main CEF pathway contributing to dark-reduction of the PQ pool. Attribution of the increased dark-reduction of PQ in OE-NTRC to enhanced activity of the NDH complex was further supported by the observation that redox state of the PQ pool in darkness was more oxidized in the OE-NTRC *ndho* line in comparison to WT and OE-NTRC (Fig. 3G). OJIP transients also showed increased dark-reduction of PQ in *ntrc* mutant when compared to WT (Fig. 3C), but it must be noted that the overall kinetics of the OJIP transient in *ntrc* differed considerably from the other lines, which may affect interpretability of the results from the pleiotropic *ntrc* knockout line.

Differences in PQ redox state could be caused by altered content of PSII or PSI complexes, the NDH complex, Cytochrome *b6f* or plastid terminal oxidase (PTOX). No significant differences were detected in the amounts of the PSII core protein D1, Cyt *b6f* subunit Cyt *f* or NDH subunits NdhS and NdhH between the studied lines, while a decrease in the amount of PGR5 and the PSI core protein PsaB, and an elevated PTOX content were detected in *ntrc* (Fig. 4).

## NTRC enhances the formation of the proton motive force during dark-to-light transitions

Reduction of plastoquinone by the thylakoid NDH complex is known to be coupled to translocation of protons to the lumen, which contributes to the formation of *pmf* and enhances ATP synthesis (Strand et al., 2017a). We therefore investigated whether formation of the *pmf* during dark-to-light transitions and in plants illuminated with different light conditions is affected by deficiency or overexpression of NTRC. The *pmf*, conductivity of the thylakoid membrane to protons ( $g_{H^+}$ ) and proportions of the *pmf* components  $\Delta pH$  and  $\Delta\Psi$  were determined by measuring absorbance changes at 515–550 nm, also known as the electrochromic shift (ECS) (Cruz et al., 2005). Upon onset of illumination at growth light intensity *pmf* was transiently elevated in WT, peaking after 15–20 seconds (Fig. 5A) and coinciding with a decrease in  $g_{H^+}$  (Fig. 5C). The initial decrease in  $g_{H^+}$  occurred despite rapid reduction of the gamma subunit of the ATP synthase ( $CF_1\gamma$ ), as after 20 s under growth light  $CF_1\gamma$  was already fully reduced (Fig. 5G) (Kramer et al., 1990). Under growth light intensity, another slight rise in *pmf* was observed after ca. 30–60 seconds in light, coinciding with P700 oxidation (Fig. 5A and 6D). Subsequently *pmf* slowly decreased to a steady state value.

In OE-NTRC the initial *pmf* increase occurred already in a few seconds after the onset of illumination, reached a higher level and decreased more slowly than in WT (Fig. 5A). This initial *pmf* increase coincided with a transient peak in P700 oxidation both in OE-NTRC and in WT (Fig. 5A). While  $g_{H^+}$  was drastically elevated in dark-adapted OE-NTRC leaves, it rapidly decreased to a level comparable to WT (Fig. 5C). The *pmf* was higher in OE-NTRC in all light intensities when compared to WT, and the differences were mainly due to elevated  $\Delta pH$  (Fig. 5E). There was no significant difference between OE-NTRC and WT in  $g_{H^+}$  under growth light level illumination apart from the enhanced conductivity in dark-adapted leaves (Fig. 5C) as shown previously (Nikkanen et al., 2016). Moreover, the PSII quantum yield (Fig. 6B) increased only slightly during early photosynthetic induction and slightly but insignificantly decreased at steady state illumination in comparison to WT, while P700 oxidation was significantly enhanced (Fig. 6D). These results strongly suggested that the increase in *pmf* in OE-NTRC derives from CEF. Despite a higher  $\Delta pH$  under growth light intensity in OE-NTRC, we observed elevated NPQ only during the first minute after the dark-to-light transition (Fig. 6A). At steady state OE-NTRC had similar NPQ to WT.

262 In *ndho*, generation of *pmf* followed similar kinetics as in WT, but its level was diminished (Fig. 5A).  
 263 In comparison to WT, thylakoid proton conductivity was increased during the 30–60 s time period (Fig.  
 264 5C) and NPQ induction was slightly delayed (Fig. 6A). However, overexpression of NTRC in *ndho*  
 265 background resulted in elevation of *pmf* during transitions from dark to growth light similarly to OE-  
 266 NTRC, except for a time period between 15–40 s after onset of illumination, where *pmf* was lowered in  
 267 OE-NTRC *ndho* in comparison to OE-NTRC (Fig. 5A). Upon dark-to light transitions the high initial  
 268 thylakoid proton conductivity decreased like in OE-NTRC, but after 10 s of illumination  $g_{H+}$  again rose  
 269 more rapidly than in OE-NTRC (Fig. 5C). As in *ndho*, NPQ induction was slightly delayed in OE-  
 270 NTRC *ndho* (Fig. 6A). In the absence of the NDH complex, NTRC overexpression was also unable to  
 271 enhance P700 oxidation during dark-to-growth light transitions, and OE-NTRC *ndho* suffered from  
 272 increased PSI acceptor side limitation in comparison to WT (Fig. 6D and 6E). This data indicates that  
 273 the enhanced capacity of the stroma in OE-NTRC to pull electrons from PSI during dark-to-light  
 274 transitions is dependent on the NDH-complex.

275 Increased activation of the NDH complex is not, however, sufficient to fully explain the elevated *pmf* in  
 276 OE-NTRC, especially immediately after dark-to-light transitions and at steady state. Therefore, we also  
 277 generated an NTRC overexpression line in the *pgr5* mutant background (OE-NTRC *pgr5*) whose  
 278 NTRC expression level was comparable to OE-NTRC (Suppl. Fig. 1B). In the *pgr5* mutant, *pmf*  
 279 generation and NPQ induction at the onset of illumination were impaired (Fig. 5B and Fig. 6A). The  
 280 secondary *pmf* rise was missing and the steady state level of *pmf* was lower than in WT, in part due to  
 281 increased  $g_{H+}$  (Fig. 5B and 5E). Absence of PGR5 did not alter the kinetics of *pmf* induction in plants  
 282 overexpressing NTRC, but the magnitude of *pmf* remained lower (Fig. 5B). At steady state, *pmf* in the  
 283 OE-NTRC *pgr5* plants did not differ from *pgr5* plants (Fig. 5B), while proton conductivity of the  
 284 thylakoid membrane was drastically increased even in comparison to *pgr5* (Fig. 5D). Moreover, PSI  
 285 acceptor side limitation was only slightly alleviated in OE-NTRC *pgr5* in comparison to *pgr5* (6E).  
 286 Interestingly, a high initial  $g_{H+}$  value and rapid generation of a *pmf* peak after onset of illumination  
 287 were observed in OE-NTRC, OE-NTRC *ndho* and OE-NTRC *pgr5* plants but missing in WT, *ndho* and  
 288 *pgr5* plants (Fig. 5A and 5B). This demonstrates that the first rapidly-induced *pmf* peak in plants  
 289 overexpressing NTRC is not caused by increased CEF.

290 Upon onset of illumination at growth light intensity, the initial *pmf* increase in *ntrc* occurred with  
 291 similar kinetics to WT, but had a lesser magnitude (Fig. 5A). The secondary *pmf* increase was absent in

*ntrc* leaves. At steady state the strength of *pmf* was comparable to WT, but contribution of  $\Delta pH$  to total *pmf* was slightly diminished (Fig. 5E–F). NPQ was however elevated (Fig. 6A), implying active  $\Delta pH$ -independent upregulation of NPQ. Decreased thylakoid conductivity to protons was observed in growth light intensity in *ntrc* (Fig. 5C). Reduction of CF<sub>1</sub> $\gamma$  is impaired in *ntrc* under low light but not in growth light (Nikkanen et al., 2016), implying that thylakoid proton conductivity is inhibited by other means. In *ntrc*, *pgr5* and OE-NTRC *pgr5* Q<sub>A</sub> was maintained in a highly reduced state during dark-to-growth light transitions (Fig. 6C). In *pgr5* and OE-NTRC *pgr5* this was due to impaired induction of NPQ (Fig. 6A), lack of photosynthetic control at Cyt *b6f* and the consequential inability to oxidize PSI (Suorsa et al., 2012) (Fig. 6D). In *ntrc*, however, high donor side limitation of PSI was measured in growth light despite high excitation pressure in the PQ pool (Fig. 6D) and decreased PsaB content (Fig. 4), suggesting inhibition of electron transfer between the PQ pool and PSI, possibly at Cyt *b6f*. Lower and higher content of PGR5 and PTOX, respectively, (Fig. 4) may assist to relax excitation pressure in the PQ pool of *ntrc* plants.

### **In fluctuating light NTRC overexpression enhances PSI yield in low light and represses thylakoid conductivity to protons upon transitions from low to high irradiance**

As it has been suggested in recent reports that NTRC is particularly important under low and fluctuating light conditions (Nikkanen et al., 2016; Carrillo et al., 2016; Thormählen et al., 2017), we next investigated *pmf* formation and photosynthetic electron transfer under these conditions. During transitions from dark to low light intensity, increased *pmf* formation was again observed in OE-NTRC, but the difference to WT was less dramatic than in growth light (Fig. 7A). PSII yield was enhanced in OE-NTRC during the transition from dark to low light (Fig. 8A), contributing to the *pmf* increase. P700 oxidation was also enhanced during dark to low light transitions (Fig. 9B), while NPQ was decreased, despite higher  $\Delta pH$  (Fig. 8B). A high PSI yield was maintained throughout the low light periods in OE-NTRC due to low acceptor side limitation (Fig. 9). Overexpression of NTRC in *ndho* background reverted these changes observed in OE-NTRC plants to levels comparable to *ndho* knockout plants, except for the increased PSII yield during dark-to-low light transitions (Fig. 7, 8 and 9), suggesting that enhanced activation of NDH-mediated CEF contributes to photosynthetic performance of OE-NTRC during dark to light transition and under low light.

Both *pgr5* and *ndho* showed impaired *pmf* generation during transitions from dark to low light, with most severe impairment occurring in *pgr5* 30–60 seconds after the onset of low illumination. (Fig. 7A and B). Notably, this is the time frame where transient NPQ and P700 oxidation are induced in WT but not in *pgr5* (Fig. 8B and 9B). In contrast, *pmf* generation in OE-NTRC *pgr5* during dark-to-low and low-to-high light transitions was recovered to WT levels (Fig. 7A) despite elevated  $g_{H+}$  especially in high light (Fig. 7D), most likely due to enhanced activity of NDH-CEF. Slightly improved tolerance to light fluctuation was also observed in OE-NTRC *pgr5* in comparison to *pgr5* as the PSI yield was better maintained in low light following the high light periods (Fig. 9A). Importantly, overexpression of NTRC improved the ability to oxidize PSI in low light even in the *pgr5* background (Fig. 9B, 9C).

Upon the switch from low to high light intensity, a transient *pmf* spike was observed in all lines (Fig. 7A), likely deriving from a sudden increase in the electric field component of *pmf* ( $\Delta\psi$ ) (Davis et al., 2016). In WT, the proton conductivity of the thylakoid membrane was downregulated (Fig. 7B and 8B). The downregulation was not due to oxidation of CF<sub>1</sub> $\gamma$ , as it remained fully reduced in high light conditions (Suppl. Fig. 3B). The downregulation of  $g_{H+}$  was even stronger in OE-NTRC upon the shift from low to high light (Fig. 7B). Despite elevated *pmf* (Fig. 7A), NPQ induction was attenuated (Fig. 8B). Overexpression of NTRC in *ndho* background decreased *pmf* generation during transitions from low to high light in comparison to the OE-NTRC line (Fig. 7A), suggesting that enhanced activation of NDH-mediated CEF contributes to the high *pmf* in OE-NTRC in these conditions. OE-NTRC *ndho* showed increased steady-state  $g_{H+}$  under high irradiance similarly to *ndho* (Fig. 7B). It is therefore likely that the elevated  $g_{H+}$  values in *ndho* and OE-NTRC *ndho* (Fig. 5 and Fig. 7) are at least partly caused by lack of NDH-mediated proton influx to the lumen.

In high light the *pgr5* mutant was unable to oxidize P700 (Fig. 9B) or to inhibit thylakoid conductivity (Fig. 7D), and the high  $g_{H+}$  led to a loss of *pmf* (Fig. 7C). The strong decrease of  $g_{H+}$  observed in OE-NTRC in high light (Fig. 7B) disappeared in OE-NTRC *pgr5*, which lacks PGR5 (Fig. 7B), suggesting that PGR5 contributes to the downregulation of thylakoid proton conductivity under these conditions. Recovery of *pmf* in high light through NTRC overexpression (Fig. 7C) was not sufficient to induce NPQ (Fig. 8B) or to control excess electron flow to PSI in *pgr5* background (Fig. 9B). This supports the hypothesis that the PGR5 protein is directly required to induce photosynthetic control at Cyt *b<sub>6</sub>f* (Suorsa et al., 2013; Tikkanen et al., 2015).

In *ntrc*, high steady state *pmf* under low light intensity (Fig. 7A) was likely caused by impaired activation of the chloroplast ATP synthase and the Calvin-Benson cycle as previously reported (Nikkanen et al. 2016, Carrillo et al. 2016). Partitioning of the *pmf* to  $\Delta pH$  and  $\Delta\Psi$  revealed that the contribution of  $\Delta\Psi$  to total *pmf* was slightly increased in *ntrc* and decreased in OE-NTRC in both low and high light (Fig. 5F). Exceptionally high NPQ was recorded in the *ntrc* line, especially at low light (Fig. 8B).

Concluding from Figures 5–9, it is evident that both the knockout and overexpression of NTRC had a distinct influence on the formation and regulation of *pmf* as well as on the induction of NPQ during transitions from dark to light and from low to high light through regulation of CEF activity and ATP synthase conductivity.

### Identification of CEF-related NTRC target proteins

Distinct effects of NTRC overexpression or deficiency on the post-illumination fluorescence rise (Fig. 2), the dark-reduction level of the plastoquinone pool (Fig. 3) and formation of *pmf* as well as on the regulation of thylakoid conductivity during dark/light transitions and low/high light transitions (Fig. 5 and 7) suggested that NTRC may either directly or indirectly regulate CEF. In order to screen for potential targets of direct NTRC-mediated regulation, we performed co-immunoprecipitation (Co-IP) assays with an antibody against NTRC, and analyzed eluates from WT, *ntrc* and OE-NTRC total leaf extracts by mass spectrometry (MS). A full list of identified peptides is provided in Supplemental Dataset 1.

The Co-IP/MS analysis revealed that among peptides that were detected in WT and OE-NTRC eluates but were absent in the eluates from *ntrc* were several proteins involved in CEF around PSI (Table 1). Most notably, five subunits of the thylakoid NDH complex; NdhH, Ndh48, NdhS, NdhU and NdhO, (in order of abundance) as well as PGR5 were identified as potential NTRC interactors. Furthermore, although Ndh45 and NdhJ were detected in *ntrc* eluates, they were notably enriched in WT and/or OE-NTRC eluates. Intriguingly, all of the NDH subunits identified are located close proximity to the proposed ferredoxin binding and oxidation site on the stromal side of the NDH complex (Yamamoto et al., 2011; Yamamoto and Shikanai, 2013; Peltier et al., 2016; Shikanai, 2016).

378 The potential interactions of NTRC with NdhS and PGR5 were further supported by positive results in  
379 bimolecular fluorescence complementation tests (BiFC). Co-expression of NTRC with both NdhS and  
380 PGR5 in *Nicotiana benthamiana* leaves resulted in YFP fluorescence that was strictly co-localized with  
381 chlorophyll autofluorescence, suggesting that it originated from the thylakoid membranes (Fig. 10).  
382 TRX-*m1* interacted with PGRL1, while no interaction capability was detected between PGRL1 and  
383 NTRC (Fig. 10).

384 To assess the potential of the CEF-related proteins identified by Co-IP/MS (Table 1) and BiFC (Figure  
385 10) to be targets of redox-regulation by TRXs, their amino acid sequences were analysed for conserved  
386 cysteine residues. Of the NDH subunits identified as putative NTRC targets by Co-IP/MS, NdhS,  
387 NdhH, Ndh48, NdhJ and Ndh45 contain cysteine residues that are conserved in angiosperms (Table 1,  
388 Suppl. Tables 2–6), and therefore could in theory be subject to thiol regulation. NdhO and NdhU do not  
389 contain conserved cysteine residues, but they likely co-precipitate with the NTRC antibody because of  
390 their interactions with NdhH and NdhS subunits of the NDH complex, respectively (Shikanai, 2016).

391 PGR5 has been shown to form redox-dependent heterodimers with PGRL1 which have been proposed  
392 to be required for acceptance of electrons from ferredoxin and for reduction PGRL1 (Hertle et al.,  
393 2013; Leister and Shikanai, 2013). The mature PGR5 polypeptide contains a single highly conserved  
394 cysteine residue (Munekage et al., 2002), which could hypothetically form an intermolecular disulfide  
395 with PGRL1 or some other partner, or be a target for S-nitrosylation or glutathionylation (Couturier et  
396 al., 2013; Zaffagnini et al., 2016). As direct determination of PGR5 redox state with the alkylation  
397 method was not feasible, we investigated if the redox state of PGRL1 is affected by NTRC deficiency  
398 or overexpression. PGRL1 contains six conserved thiol-sensitive cysteine residues that form inter- and  
399 intramolecular disulfides (Petroutsos et al., 2009; Hertle et al., 2013). We observed that PGRL1 was  
400 mostly oxidized in dark-adapted leaves, but underwent a transient reduction during approximately 60  
401 seconds of illumination with growth light (Suppl. Fig. 3). This corresponds with the timescale of NPQ  
402 induction (Fig. 6B), as well as with the transient increase in *pmf* and decrease in *g<sub>H+</sub>* during dark-to-  
403 light transitions (Fig. 5A and 5B). No significant difference to WT in PGRL1 reduction or protein  
404 content was detected in OE-NTRC (Suppl. Fig. 3, Fig. 4). PGR5 content of thylakoid membranes was,  
405 however, decreased in *ntrc* by 40% in comparison to WT (Fig. 4), in line with observations in a  
406 previous study (Yoshida and Hisabori, 2016).

## DISCUSSION

The role of CEF around PSI in plant acclimation to fluctuating light conditions has attracted great attention during the past 10 years. Importance of CEF likely relies in its capacity to maintain redox homeostasis in chloroplasts upon fluctuations in light intensity and during dark-to-light transitions (Yamori et al., 2016; Suorsa et al., 2016; Strand et al., 2016b). Plastidial thioredoxin systems, on the other hand, are crucial regulators of chloroplast metabolic reactions in the stroma. It has, however, remained unclear whether the thioredoxin-related redox regulation is also involved in the achievement of CEF-mediated redox homeostasis upon exposure of plants to changing light intensities. To this end, we applied here an *in-vivo* approach to investigate whether NTRC contributes directly to regulation of CEF pathways in chloroplasts.

In-depth analyses of NTRC overexpression lines in respect to thylakoid functional properties provided strong evidence that NTRC indeed is involved in the regulation of CEF in the thylakoid membrane. Compelling support for NTRC-induced activation of the NDH complex was obtained by analyzing thylakoid CEF-related functions in NTRC overexpression lines made on the backgrounds of *ndho* (OE NTRC *ndho*) and *pgr5* (OE NTRC *pgr5*), incapable of performing NDH- and PGR-dependent CEF, respectively. Distinct effect of NTRC overexpression on the post-illumination rise of chlorophyll *a* fluorescence, the redox state of the plastoquinone pool in darkness as well as on generation of the *pmf* and oxidation of P700 upon dark-to-light transitions and sudden increases in light intensity demonstrated the control of NDH-dependent CEF by NTRC (Figs. 2, 3, 5, 6, 7). Furthermore, evidence for a direct effect of NTRC on the NDH activity was obtained by identification of NDH subunits in a close proximity of the ferredoxin binding site as potential NTRC interactors (Table 1, Fig. 10, Suppl. Dataset 1, Suppl. tables 2–6). Although several NDH subunits were detected by Co-IP/MS, most likely only one or few of these subunits are genuine NTRC targets. The others likely co-precipitate with the NTRC antibody due to reciprocal interactions of the NDH subunits on the stromal side of the thylakoid membrane (Shikanai, 2016; Peltier et al., 2016). Existence of a thiol-regulated component in the ferredoxin binding site would provide a mechanism for dynamic control of the ferredoxin:plastoquinone oxidoreductase activity of the complex in response to fluctuations in light conditions. Redox-regulation of the NDH complex would allow rapid adjustment of *pmf* and non-photochemical quenching as well as a maintenance of redox balance between the electron transfer chain and the electron sink capacity of stromal acceptors, most importantly the CBC. In high light, less

active NDH could prevent the reverse function of the complex (i.e. oxidization of PQ to reduce ferredoxin and transfer of H<sup>+</sup> from lumen to stroma) in conditions of high ΔpH and a reduced PQ pool (Strand et al., 2017a).

Notably, the overexpression of NTRC also affects the function of PGR5. Nevertheless, the effect is not necessarily related to the putative role of PGR5 in CEF. Our results, more likely, support the hypothesis (Avenson et al., 2005; Tikkanen et al., 2015; Kanazawa et al., 2017; Armbruster et al., 2017) that PGR5 controls the proton conductivity of the thylakoid membrane that, consequently, affects the generation of *pmf*.

The photosynthetic parameters measured for the *ntrc* knockout plants were not always in line with the results obtained with NTRC overexpressing plants (Fig. 3). In short photoperiod the *ntrc* plants have a highly pleiotropic phenotype (Fig. 4, Supl. Fig. 2) (Kirchsteiger et al., 2009; Pulido et al., 2010; Thormählen et al., 2015; Naranjo et al., 2016; Nikkanen et al., 2016; Pérez-Ruiz et al., 2017) that complicates the interpretation of results from the *ntrc* line. Thus the OE-NTRC line, whose visible phenotype and development are not considerably dissimilar to WT, provides a more reliable platform to examine the direct effects of NTRC on specific plastidial processes.

### **Regulation of the *pmf* and redox homeostasis via NDH and NTRC during changes in light conditions**

Overexpression of NTRC caused elevated *pmf* under all light conditions, while no significant changes were observed in PSII electron transfer rate or thylakoid proton conductivity in comparison to WT (Figures 5–8). These results strongly suggest that the elevation of *pmf* derives from enhanced CEF. Increased P700 oxidation during dark-to-light transitions in OE-NTRC was fully reverted in OE-NTRC *ndho*, and a lack of NDH also delayed the ability to oxidize P700 during the high light phases in fluctuating light (Fig. 6, 9). It is therefore evident that the NDH complex regulates the trans-thylakoid *pmf* as well as the redox balance between the electron transfer chain and the stroma, and this regulation is under the control of the stromal TRX systems, with our results suggesting a specific role for the NTRC system.

While our results demonstrate enhancement of the NDH-dependent CEF by NTRC overexpression (Fig. 2), earlier studies have revealed an inhibition of NDH-dependent CEF upon TRX-*m4* overexpression and, conversely, an enhancement in *trxm4* mutants (Courteille et al., 2013). Thus, it is conceivable that the two chloroplast TRX systems regulate CEF in an antagonistic way, although it remains to be elucidated how such regulation might be mechanistically accomplished. We propose that in low light and upon sudden changes in the light intensity, NTRC is crucial for activation of the NDH-dependent CEF, while the TRX-*m4* -dependent inhibition of NDH-CEF requires higher light intensity or longer duration of illumination. Sustained moderate to high-light illumination is required to fully activate the FTR-dependent TRX system (reviewed in Geigenberger et al. 2017) that possibly contributes to downregulation of NDH. In OE-NTRC the NDH-dependent CEF is constitutively active in light, which contributes to elevated *pmf* in all light intensities. Upon transition from dark to low light, there is less difference between OE-NTRC and WT in terms of *pmf* formation (Fig. 7), because in those conditions the NTRC-mediated activation of NDH occurs similarly in WT and OE-NTRC.

The NDH complex translocates protons from the stroma to the lumen not only via Cyt *b6f*, but also functions as a proton pump with a 2 H<sup>+</sup>/e<sup>-</sup> stoichiometry (Strand et al., 2017a). NDH-mediated CEF therefore contributes relatively more to  $\Delta$ pH generation and consequently to ATP synthesis and NPQ induction than the PGR-dependent pathway. It has been postulated that the NDH complex is unlikely responsible for CEF during the early induction phase of photosynthesis, due to a low concentration of the complex in thylakoids in relation to the total PSI content (Joliot and Joliot, 2002). However, the NDH complex forms functional CEF-supercomplexes with PSI in stroma thylakoids (Peng et al., 2008), and a single NDH complex can bind up to six PSI complexes (Yadav et al., 2017), indicating that even a relatively low NDH content may have a significant impact on *pmf* generation.

### **Redox-regulation of the PGR-dependent CEF pathway and ATP synthase**

Increased activation of NDH-CEF is not alone sufficient to explain all observed changes of *pmf* in OE-NTRC plants. When compared to WT, *pmf* remained elevated in OE-NTRC *ndho* during the first seconds of photosynthetic induction and at steady state in growth and high light (Fig. 5A and 7A). These results could be explained by activation of PGR-dependent CEF as well in plants overexpressing NTRC. Stromal thiol redox state has been previously suggested to control the PGR-dependent CEF by

493 a component that has a midpoint redox potential of -310 (Hertle et al., 2013; Strand et al., 2016a). It has  
 494 also been proposed that *m*-type TRXs, with redox potentials between -357 and -312 mV (Collin et al.,  
 495 2003; Yoshida et al., 2015), reduce an intermolecular disulfide in PGRL1 homodimers, and  
 496 subsequently, the released monomeric PGRL1 may function as the ferredoxin-plastoquinone reductase  
 497 (Hertle et al., 2013). Here we confirm the previously reported transient reduction of PGRL1 during  
 498 dark-to-light transitions (Hertle et al., 2013), but NTRC overexpression does not intervene in the  
 499 reduction (Suppl. Fig. 3). Moreover, TRX-*m*1 but not NTRC interacts with PGRL1 in BiFC (Fig. 10).  
 500 Our results thus support the hypothesis that TRX-*m* is a primary reductant of PGRL1. Crosstalk  
 501 between NTRC and FTR-dependent systems (Toivola et al., 2013; Thormählen et al., 2015; Nikkanen  
 502 et al., 2016), and the interaction of NTRC with TRX-*m*1 in BiFC (Nikkanen et al., 2016), further  
 503 support the interpretation that the activation of PGR-dependent CEF is indirectly increased in NTRC-  
 504 overexpressing plants through enhancement of TRX-*m* reduction. This would also be in line with the  
 505 steady state *pmf* increase observed in OE-NTRC *ndho* in comparison to WT (Fig. 5A and 7A).

506 Alternatively, NTRC overexpression may affect the function of PGR5 in a way that is independent of  
 507 its involvement in CEF. Redox regulation of PGR5 may occur to control its association with the ATP  
 508 synthase during dark-to-light and low-to-high light transitions, and thereby inhibit the conductivity of  
 509 the ATP synthase in an unknown mechanism, as suggested earlier (Avenson et al., 2005; Tikkanen et  
 510 al., 2015; Kanazawa et al., 2017; Armbruster et al., 2017). Such a mechanism would result in  
 511 acidification of the lumen and induction of NPQ, allowing dissipation of excess excitation energy from  
 512 the electron transfer chain until CBC is activated. This hypothesis is supported by the impaired abilities  
 513 of *pgr5* and OE-NTRC *pgr5* to control thylakoid conductivity at early stages of dark-light transitions  
 514 and upon transitions to high light intensities (Avenson et al., 2005, Fig. 5 and Fig. 7). Furthermore, the  
 515 elevated NTRC content in leaves accelerated the decline of the thylakoid proton conductivity upon  
 516 increases in light intensity (Fig. 7B), suggesting that NTRC controls the PGR5-dependent down-  
 517 regulation of proton efflux from lumen. This is supported by the identification of PGR5 as a potential  
 518 NTRC interactor (Table 1, Fig. 4, Fig. 10).

519 However, the absence of the NDH complex, albeit to a lesser extent than the absence of PGR5, also  
 520 causes an impaired ability to decrease thylakoid proton conductivity in high light (Fig. 7). Thus, it is  
 521 likely that proton influx to the lumen caused by proton pumping in CEF decreases the measured value  
 522 of  $g_{H^+}$ . This could be expected to have a particularly significant impact during dark-to-light and low-to-

high light transitions when the fraction of CEF from total electron flow is high (Joliot and Joliot, 2002; Fan et al., 2007), and in mutants, where CEF capacity is altered (Livingston et al., 2010; Wang et al., 2015; Suorsa et al., 2016). Therefore, the deficiency of the NDH and PGR-dependent pathways of CEF in *ndho* and *pgr5* backgrounds, respectively, may contribute to the high  $g_{H+}$  values measured in those lines. Therefore, a hypothesis in which the rapid repression of  $g_{H+}$  in OE-NTRC derives, at least partially, from the enhanced activity of the CEF pathways, cannot be discarded.

The initial strong *pmf* increase in OE-NTRC after onset of growth light illumination was evident also in both the OE-NTRC *ndho* and OE-NTRC *pgr5* plants (Fig. 5A and B) indicating that this *pmf* peak is not caused by CEF. More likely, the initial *pmf* results from dark-activation of the CBC enzymes in plants overexpressing NTRC (Nikkanen et al. 2016), which provides an enhanced ability of the stroma to accept electrons from the PETC upon dark-to light transition and consequently enhances proton pumping to the lumen.

## **Cooperative regulation of photosynthetic electron transfer and carbon fixation by chloroplast thioredoxin systems**

Light-dependent reductive activation of the ATP synthase, the CBC and the NADP-malate dehydrogenase (NADP-MDH) by TRXs has been well established for several decades (reviewed in (Buchanan, 2016). More recently, knowledge of TRX-mediated control has been extended to various regulatory and photoprotective mechanisms of photosynthesis, including regulation of state transitions (Rintamäki et al., 2000; Shapiguzov et al., 2016), NPQ (Hall et al., 2010; Brooks et al., 2013; Naranjo et al., 2016; Da et al., 2017) and CEF (Courteille et al., 2013; Hertle et al., 2013; Strand et al., 2016a). We propose here a model, comprising a cooperative function of the two chloroplast TRX systems with distinct reductants and redox potentials that allows the maintenance of redox homeostasis between the two photosystems and stromal metabolism during fluctuations in light conditions. This is achieved through dynamic regulation of the activities of the ATP synthase, NPQ, the NDH complex, PGRL1/PGR5 as well as the LHCII kinase STN7 by reversible thiol modifications. We propose a specific role for NTRC in regulating NDH-CEF, the ATP synthase and CBC enzymes in low light, dark-to-light transitions and during sudden increases in light intensity, as schematically depicted in Fig. 11.

552 In darkness, NDH is partially activated by NTRC, and moderate chlororespiration from NDH to PTOX  
 553 occurs. Due to inactivity of the ATP synthase and proton pumping activity of NDH, a weak proton  
 554 gradient over the thylakoid membrane is established. Redox-regulated CBC enzymes are inactive,  
 555 causing PC and P700 to be reduced due to lack of acceptors. In OE-NTRC, chlororespiration via NDH  
 556 to the PQ pool is increased due to enhanced activation of NDH. This leads to increased protonation of  
 557 the lumen and reduction of the PQ pool. Overexpressed NTRC reduces CF<sub>I</sub>γ, partially activating the  
 558 ATP synthase and making it leaky to H<sup>+</sup>. CBC enzymes are also partially activated by NTRC.

559 Upon transition from dark to low light, the ATP synthase is fully and CBC enzymes partially reduced  
 560 by NTRC in WT plants. This causes, however, a lag phase where a lack of stromal acceptors is limiting  
 561 electron transfer, leading to reduction of the PQ pool. NTRC contributes to activation of NDH-  
 562 dependent CEF, which alleviates electron pressure at PSI and transiently increases ΔpH and induces  
 563 NPQ. In OE-NTRC P700 and PC are effectively oxidized upon onset of low illumination, as the  
 564 acceptor side limitation is negligible due to fully active NDH-dependent CEF, ATP synthase and  
 565 redox-activated CBC enzymes. This results in an elevated ΔpH and faster induction of NPQ in  
 566 comparison to WT at the initial phase of illumination. At steady state NPQ is lower than in WT despite  
 567 of high ΔpH, suggesting downregulation of NPQ by thioredoxin via a ΔpH-independent mechanism, as  
 568 reported previously by Brooks et al. (2013).

569 When a leaf shifts from low to high irradiance, both TRX systems become fully active, and the CBC  
 570 enzymes as well as PGR-dependent CEF are fully activated. NTRC affects PGR5-dependent down-  
 571 regulation of thylakoid conductivity to protons, possibly through direct PGR5-mediated inhibition of  
 572 the ATP synthase, which contributes to accumulation of protons in the lumen. Consequently, NPQ and  
 573 inhibition of electron transfer at Cyt *b6f* are induced. Electrons are effectively pulled from PSI, and the  
 574 donor side is limiting electron transfer. In OE-NTRC, increased reduction of PGR5 likely leads to  
 575 stronger inhibition of thylakoid proton conductivity. This, together with proton pumping by constantly  
 576 active NDH and possibly through increased TRX-*m*-mediated activation of the PGR-dependent  
 577 pathway, results in high ΔpH. NPQ is however lower than in WT due to ΔpH-independent  
 578 downregulation of NPQ by overexpressed NTRC.

579

580

## METHODS

### Plant material and growth conditions

Experiments have been done with *Arabidopsis thaliana* wild type (WT) lines of the Columbia ecotype (Col-0 and Col-*gll*), and with the following transgenic lines: NTRC overexpression line (Toivola et al., 2013), T-DNA knockout mutants of NTRC (At2g41680, SALK\_096776) (Lepistö et al., 2009), *ndho* (At1g74880, SALK\_068922) (Rumeau et al., 2005) and STN7 (AT1G68830, SALK\_073254) (Bellafiore et al., 2005) as well as the *pgr5* mutant (AT2G05620) (Munekage et al., 2002). The plants were grown in a photoperiod of 8 h light / 16 h darkness at 23 °C under 200  $\mu\text{mol}$  of photons  $\text{m}^{-2} \text{s}^{-1}$  for all experiments except for the measurements shown in Suppl. Fig. 2, for which plants were grown in a 12 h / 12 h photoperiod under 130  $\mu\text{mol}$   $\text{m}^{-2} \text{s}^{-1}$ . Wild type tobacco (*Nicotiana benthamiana*) plants used in BiFC tests were grown under 130  $\mu\text{mol}$  photons  $\text{m}^{-2} \text{s}^{-1}$  at 23 °C in a 16 h light/8 h dark photoperiod. The OE-NTRC *ndho* and OE-NTRC *pgr5* lines were generated by *Agrobacterium tumefaciens* and floral dipping –mediated transformation of the *ndho* knockout and *pgr5* mutant lines, respectively, with the NTRC overexpression construct as described previously (Toivola et al., 2013). The OE-NTRC *ndho* and OE-NTRC *pgr5* plants used in the experiments were heterozygous T2 generation plants that were selected on agar plates with 0.5X Murashige-Skoog medium (MS) (Murashige and Skoog, 1962) and 50  $\mu\text{g}/\text{ml}$  kanamycin. The plants were subsequently transferred to soil and grown in a 8 h light / 16 h darkness photoperiod at 23 °C under 200  $\mu\text{mol}$  of photons  $\text{m}^{-2} \text{s}^{-1}$  for four weeks before usage in the experiments. As control, OE-NTRC plants were similarly selected on kanamycin-containing plates while WT Col-0 and WT Col-*gll* (ecotype of the *pgr5* mutant) plants were grown on 0.5X MS-agar plates without antibiotics for an equivalent time.

### Measurement of Chlorophyll a fluorescence and P700 oxidation changes

The post-illumination chlorophyll a fluorescence rise (PIFR) was measured from detached leaves with the Multicolor-PAM fluorometer (Walz). A 480 nm measuring beam at an intensity of 0.2  $\mu\text{mol}$  photons  $\text{m}^{-2} \text{s}^{-1}$  was used to measure fluorescence changes after illumination of dark-adapted (30 min) leaves with 67  $\mu\text{mol}$  photons  $\text{m}^{-2} \text{s}^{-1}$  of white actinic light for 500 seconds, with saturating pulses in the beginning and at 400 s to determine  $F_m$  and  $F_m'$ . The actinic light was then switched off and the changes in chlorophyll a fluorescence in the dark were observed for 300 s. A brief pulse of far red light

was then given to fully oxidize the PQ pool, and the subsequent re-reduction PQ pool was detected through a rise in Chl fluorescence.

The OJIP transients were recorded with the Multicolor-PAM from dark-adapted (30 min) leaves and from leaves pre-illuminated with far red light (intensity setting 15) for 6 s, according to the method described by (Toth et al., 2007). A saturating pulse of 3000  $\mu\text{mol photons m}^{-2} \text{s}^{-1}$  and measuring light at 440 nm were used in the measurements.

The Dual-PAM-100 was used to simultaneously record the Chl a fluorescence and 870–820 nm absorbance changes during transitions from dark to 166  $\mu\text{mol photons m}^{-2} \text{s}^{-1}$  (Fig. 6) and during a light regime, where a 620 nm AL fluctuates between 39 and 825  $\mu\text{mol photons m}^{-2} \text{s}^{-1}$  (Fig. 8 and Fig. 9). Saturating pulses were administered at 10 or 15 s intervals for the measurements in Fig. 6 and at 15 s intervals for the first minute after onset of illumination, and at 20 s intervals thereafter for Fig. 8 and Fig. 9. Because *ntrc* leaves are very small in size and low in chlorophyll content, it was in some cases necessary to record from two or three leaves simultaneously to obtain a P700 signal of sufficient quality. The parameters shown were calculated with the Dual-PAM-100 software and are based on (Kramer et al., 2004).

## Measurement of electrochromic shift (ECS)

In order to measure the strength and formation kinetics of the proton motive force (*pmf*), changes in the electrochromic shift (ECS, P515) signal were recorded with the Dual-PAM-100 and the P515/535 accessory module (Walz) (Schreiber and Klughammer, 2008). A dual beam difference signal at 550–515 nm was used to avoid distortion of results by scattering effects. For the dark-to-light and low-to-high light transition measurements in Figures 5 and 7, plants were first dark-adapted for 30 min. A single-turnover (20  $\mu\text{s}$ ) saturating flash of 14000  $\mu\text{mol photons m}^{-2} \text{s}^{-1}$  was then applied to obtain ECS<sub>ST</sub>, a maximum absorbance change value that was used to normalize all results to account for differences in leaf thickness and chlorophyll content between individual leaves and lines (Kramer and Crofts, 1989). The obtained values of ECS<sub>ST</sub> were in good correlation with the chlorophyll content in OE-NTRC and *ntrc* lines reported previously (Toivola et al., 2013). In order to distinguish the light-induced ECS change (ECS<sub>T</sub>) from signal drift and baseline change attributable to zeaxanthin formation (Klughammer et al., 2013), frequent dark intervals of 250 ms were applied during AL illumination.

ECS<sub>T</sub> was calculated as the difference between total ECS in light and an Y<sub>0</sub> value obtained from the first-order exponential fit to the decay kinetics of the ECS signal during a dark interval. Total *pmf* was then calculated as ECS<sub>T</sub>/ECS<sub>ST</sub>. The g<sub>H+</sub> parameter, describing thylakoid membrane conductivity to protons, was calculated as the inverse of the time constant of a first-order exponential fit to ECS decay kinetics during a dark interval (Cruz et al., 2001; Avenson et al., 2005; Cruz et al., 2005). A green measuring light at a 2000 Hz pulse frequency was used in all ECS measurements. Partitioning of total *pmf* to its components ΔpH and ΔΨ was performed as described by (Cruz et al., 2001).

### **Protein extraction, alkylation of thiols and SDS-PAGE**

Proteins and thylakoids were isolated as previously described (Lepistö et al., 2009), while chlorophyll content was determined according to (Porra et al., 1989) and protein content with the Bio-Rad Protein Assay kit. For determination of the redox states of TRX-regulated proteins, leaf proteins were precipitated with trichloroacetic acid (TCA) and free thiols in proteins alkylated with N-ethylmaleimide (NEM, Sigma-Aldrich). After alkylation protein disulfides were reduced with dithiothreitol (DTT, Sigma-Aldrich) and subsequently produced thiols were alkylated with methoxypolyethylene glycol maleimide M<sub>n</sub> 5000 (MAL-PEG, Sigma-Aldrich) as described earlier (Nikkanen et al., 2016). Sodium dodecyl sulfate polyacrylamide gel electrophoresis (SDS-PAGE) and immunoblotting was performed as reported in (Nikkanen et al., 2016). For running the MAL-PEG samples pre-cast 4-20% Mini-PROTEAN TGX gels (Bio-Rad) were used, except for the gel in Fig. 1B, Suppl. Fig. 1A and Suppl. Fig. 3A, where a 12% polyacrylamide gel was used. PVDF membranes were probed with antibodies raised against NTRC (Lepistö et al., 2009), D1 (Research Genetics, Inc (Thermo Fisher)), PsaB (Agrisera, AS10 695), Cyt *f* (kindly provided by L. Zhang), PTOX (kindly provided by M. Kuntz), NdhH (Agrisera), NdhS (Agrisera), CF<sub>1</sub>γ (Agrisera, AS08 312), PGRL1 (Agrisera, AS10 725), PGR5 (Agrisera) or phosphothreonine (P-Thr) (New England Biolabs). Membranes were then treated with a horseradish peroxidase (HRP)-conjugated goat anti-rabbit secondary antibody (Agrisera, AS09 602) for 2 h. All immunoblots shown are representative of at least 3 replicate experiments. Quantifications of protein content shown in Fig. 4 were performed using the ImageJ software (Schneider et al., 2012) and normalized according to the intensity of Li-Cor Revert Total Protein Stain. Statistical significance was

determined using two-tailed Student's T-tests for unequal variances with p-values below 0.05 interpreted as statistically significant.

## **Co-immunoprecipitation and Mass spectrometry**

Co-immunoprecipitation (Co-IP) was performed from WT, *ntrc* and OE-NTRC total leaf extracts using the Pierce Co-IP kit (Thermo-Fisher) and an NTRC-specific antibody as described previously (Nikkanen et al., 2016). Co-IP eluates were denatured and purified by SDS-PAGE in a 6% acrylamide gel with 6 M urea, subjected to in-gel tryptic digestion and the extracted peptides analyzed with the Q Exactive Hybrid Quadrupole-Orbitrap mass spectrometer (Thermo-Fisher Scientific) in DDA mode as previously described (Trotta et al., 2016). MS/MS spectra were analyzed with an in-house installation of Mascot (v.2.4) (Matrix Science) search engine and analyzed with Proteome Discoverer (v.1.4) Software (Thermo Scientific), restricting the search to the non-redundant database TAIR10 supplemented with most common laboratory contaminants (Trotta et al., 2016). Peptides were validated by Decoy Database Search, with target false discovery rates (FDR) set to be below 0.01 (strict) or below 0.05 (relaxed).

## **BiFC tests**

Bimolecular fluorescence complementation tests (BiFC) were performed as described in (Nikkanen et al., 2016). For the current study, coding sequences of PGR5, PGRL1a and NdhS obtained from Arabidopsis Biological Resource Center (ABRC) were cloned into pSPYNE-35S and pSPYCE-35S binary vectors (Walter et al., 2004), and the resulting constructs were checked by sequencing. Primer sequences used for cloning are listed in Suppl. Table 7. Imaging of YFP and chlorophyll autofluorescence from *N. benthamiana* leaves infiltrated with *Agrobacterium tumefaciens* strain GV3101 carrying the appropriate binary vectors was performed with a Zeiss LSM780 laser scanning confocal microscope at 3 days after infiltration. The negative result between PGRL1:YFP-N and NTRC:YFP-C also serves as a negative control.

## 694 **Multiple alignment of amino acid sequences**

695 Amino acid sequences of NdhH, Ndh48, NdhS, NdhJ and Ndh45 in *Arabidopsis thaliana* and, as  
696 available, in *Populus trichocarpa*, *Vitis vinifera*, *Glycine max*, *Solanum lycopersicum*, *Oryza sativa*,  
697 *Sorghum bicolor*, *Brachypodium distachion*, *Physcomitrella patens*, *Selaginella moellendorffii* and  
698 *Synechocystis PCC 6803* were obtained from the UniProtKB database and aligned with the Clustal  
699 Omega 1.2.4 online alignment tool (Sievers et al., 2011) using default settings.

700

## 701 **Accession Numbers**

702 The Arabidopsis Genome Initiative locus identifiers (AGI) used in this paper are listed in Table 1,  
703 Suppl. Tables 2–7 and Suppl. Dataset 1.

704

## 705 **Supplemental Data**

706 Supplemental Figure 1. NTRC redox state in different light conditions in OE-NTRC and level of  
707 NTRC expression in NTRC overexpression lines.

708 Supplemental Figure 2. Post-illumination fluorescence rise in dark-adapted WT, OE-NTRC and *ntrc*  
709 plants grown in a 12 h/12 h photoperiod.

710 Supplemental Figure 3. *In vivo* redox states of PGRL1 and CF<sub>I</sub>γ during changes in light conditions.

711 Supplemental Table 1. Parameters determined from OJIP transients.

712 Supplemental Table 2. Multiple alignment of NdhS amino acid sequences.

713 Supplemental Table 3. Multiple alignment of NdhH amino acid sequences.

714 Supplemental Table 4. Multiple alignment of Ndh48 amino acid sequences.

715 Supplemental Table 5. Multiple alignment of NdhJ amino acid sequences.

716 Supplemental Table 6. Multiple alignment of Ndh45 amino acid sequences.

717 Supplemental Table 7. Primers used for cloning of BiFC constructs.

Supplemental Dataset 1. MS/MS identification of peptides in Co-IP eluates.

## ACKNOWLEDGEMENTS

We thank Jesse Ojala for assistance with the experiments, Esa Tyystjärvi for the invaluable advice for PIFR measurements, Sari Järvi and Marjaana Suorsa for antibodies and advice on their use, Alexandrina Stirbet for expert advice on measurement of OJIP transients, and Mika Keränen, Kurt Ståhle and Tapio Ronkainen for technical assistance. This work was funded by the Academy of Finland Grants 276392 (to E.R.) and 307335 (the Center of Excellence in Molecular Biology of Primary Producers to E-M.A.) and by the Doctoral Program in Molecular Life Sciences in the University of Turku Graduate School (to L.N.).

## AUTHOR CONTRIBUTIONS

L.N. and E.R. designed the research, L.N., J.T., and A.T. performed the research, L.N., J.T., A.T., M.T., and E.R. analyzed the data, L.N. and E.R. wrote the article with input from E-M.A., M.T., A.T., M.G.D., and J.T.

## 742 REFERENCES

- 743 Allorement, G., Osorio, S., Vu, J.L., Falconet, D., Jouhet, J., Kuntz, M., Fernie, A.R., Lerbs-Mache, S.,  
744 Macherel, D., Courtois, F., and Finazzi, G. (2015). Adjustments of embryonic photosynthetic activity  
745 modulate seed fitness in *Arabidopsis thaliana*. *New Phytol.* 205, 707-719.
- 746 Armbruster, U., Correa Galvis, V., Kunz, H.H., and Strand, D.D. (2017). The regulation of the  
747 chloroplast proton motive force plays a key role for photosynthesis in fluctuating light. *Curr. Opin.*  
748 *Plant Biol.* 37, 56-62.
- 749 Armbruster, U., Carrillo, L.R., Venema, K., Pavlovic, L., Schmidtman, E., Kornfeld, A., Jahns, P.,  
750 Berry, J.A., Kramer, D.M., and Jonikas, M.C. (2014). Ion antiport accelerates photosynthetic  
751 acclimation in fluctuating light environments. *Nature Comm.* 5, 5439.
- 752 Avenso, T., Cruz, J., Kanazawa, A., and Kramer, D. (2005). Regulating the proton budget of higher  
753 plant photosynthesis. *Proc. Natl. Acad. Sci. U. S. A.* 102, 9709-9713.
- 754 Bailey, S., Walters, R.G., Jansson, S., and Horton, P. (2001). Acclimation of *Arabidopsis thaliana* to  
755 the light environment: the existence of separate low light and high light responses. *Planta* 213, 794-801.
- 756 Balsera, M., Uberegui, E., Schürmann, P., and Buchanan, B.B. (2014). Evolutionary Development of  
757 Redox Regulation in Chloroplasts. *Antioxid. Redox Signal.* 21, 1327-1355.
- 758 Bellafiore, S., Barneche, F., Peltier, G., and Rochaix, J. (2005). State transitions and light adaptation  
759 require chloroplast thylakoid protein kinase STN7. *Nature* 433, 892-895.

760 Breyton, C., Nandha, B., Johnson, G.N., Joliot, P., and Finazzi, G. (2006). Redox modulation of cyclic  
761 electron flow around photosystem I in C3 plants. *Biochemistry (N. Y. )* 45, 13465-13475.

762 Brooks, M.D., Sylak-Glassman, E.J., Fleming, G.R., and Niyogi, K.K. (2013). A thioredoxin-like/beta-  
763 propeller protein maintains the efficiency of light harvesting in Arabidopsis. *Proc. Natl. Acad. Sci. U.*  
764 *S. A.* 110, E2733-40.

765 Buchanan, B.B. (2016). The Path to Thioredoxin and Redox Regulation in Chloroplasts. 67, 1-24.

766 Carrillo, L.R., Froehlich, J.E., Cruz, J.A., Savage, L.J., and Kramer, D.M. (2016). Multi-level  
767 regulation of the chloroplast ATP synthase: the chloroplast NADPH thioredoxin reductase C (NTRC)  
768 is required for redox modulation specifically under low irradiance. *Plant J.* 87, 654-663.

769 Collin, V., Issakidis-Bourguet, E., Marchand, C., Hirasawa, M., Lancelin, J., Knaff, D., and Miginiac-  
770 Maslow, M. (2003). The Arabidopsis plastidial thioredoxins - New functions and new insights into  
771 specificity. *J. Biol. Chem.* 278, 23747-23752.

772 Courteille, A., Vesa, S., Sanz-Barrio, R., Cazale, A., Becuwe-Linka, N., Farran, I., Havaux, M., Rey,  
773 P., and Rumeau, D. (2013). Thioredoxin m4 Controls Photosynthetic Alternative Electron Pathways in  
774 Arabidopsis. *Plant Physiol.* 161, 508-520.

775 Couturier, J., Chibani, K., Jacquot, J., and Rouhier, N. (2013). Cysteine-based redox regulation and  
776 signaling in plants. *Front. Plant Sci.* 4, 105.

777 Cruz, J., Sacksteder, C., Kanazawa, A., and Kramer, D. (2001). Contribution of electric field ( $\Delta$   
778  $\psi$ ) to steady-state transthylakoid proton motive force (pmf) in vitro and in vivo. Control of pmf  
779 parsing into  $\Delta$   $\psi$  and  $\Delta$  pH by ionic strength. *Biochemistry (N. Y. )* 40, 1226-1237.

780 Cruz, J., Avenson, T., Kanazawa, A., Takizawa, K., Edwards, G., and Kramer, D. (2005). Plasticity in  
781 light reactions of photosynthesis for energy production and photoprotection. *J. Exp. Bot.* 56, 395-406.

782 Da, Q., Sun, T., Wang, M., Jin, H., Li, M., Feng, D., Wang, J., Wang, H., and Liu, B. (2017). M-type  
783 thioredoxins are involved in the xanthophyll cycle and proton motive force to alter NPQ under low-  
784 light conditions in Arabidopsis. *Plant Cell Rep.*

785 DalCorso, G., Pesaresi, P., Masiero, S., Aseeva, E., Schuenemann, D., Finazzi, G., Joliot, P., Barbato,  
786 R., and Leister, D. (2008). A complex containing PGRL1 and PGR5 is involved in the switch between  
787 linear and cyclic electron flow in Arabidopsis. *Cell* 132, 273-285.

788 Davis, G.A., Kanazawa, A., Schoettler, M.A., Kohzuma, K., Froehlich, J.E., Rutherford, A.W., Satoh-  
789 Cruz, M., Minhas, D., Tietz, S., Dhingra, A., and Kramer, D.M. (2016). Limitations to photosynthesis  
790 by proton motive force-induced photosystem II photodamage. *eLife* 5, e16921.

791 Demmig-Adams, B., Cohu, C.M., Muller, O., and Adams, W.W.,3rd (2012). Modulation of  
792 photosynthetic energy conversion efficiency in nature: from seconds to seasons. *Photosynth Res.* 113,  
793 75-88.

794 Fan, D., Nie, Q., Hope, A.B., Hillier, W., Pogson, B.J., and Chow, W.S. (2007). Quantification of  
795 cyclic electron flow around Photosystem I in spinach leaves during photosynthetic induction.  
796 *Photosynthesis Res.* 94, 347-357.

797 Geigenberger, P., Thormählen, I., Daloso, D.M., and Fernie, A.R. (2017). The Unprecedented  
798 Versatility of the Plant Thioredoxin System. *Trends Plant Sci.* 22, 249-262.

799 Gollan, P.J., Lima-Melo, Y., Tiwari, A., Tikkanen, M., and Aro, E. (2017). Interaction between  
800 photosynthetic electron transport and chloroplast sinks triggers protection and signalling important for  
801 plant productivity. *Philos Trans R Soc Lond B Biol Sci* 372, , doi/10.1098/rstb.2016.0390.

802 Gotoh, E., Matsumoto, M., Ogawa, K., Kobayashi, Y., and Tsuyama, M. (2010). A qualitative analysis  
803 of the regulation of cyclic electron flow around photosystem I from the post-illumination chlorophyll  
804 fluorescence transient in Arabidopsis: a new platform for the in vivo investigation of the chloroplast  
805 redox state. *Photosynthesis Res.* 103, 111-123.

806 Grieco, M., Tikkanen, M., Paakkarinen, V., Kangasjarvi, S., and Aro, E.M. (2012). Steady-state  
807 phosphorylation of light-harvesting complex II proteins preserves photosystem I under fluctuating  
808 white light. *Plant Physiol.* 160, 1896-1910.

809 Hall, M., Mata-Cabana, A., Akerlund, H.E., Florencio, F.J., Schroder, W.P., Lindahl, M., and  
810 Kieselbach, T. (2010). Thioredoxin targets of the plant chloroplast lumen and their implications for  
811 plastid function. *Proteomics* 10, 987-1001.

812 Hallin, E.I., Guo, K., and Åkerlund, H. (2015). Violaxanthin de-epoxidase disulphides and their role  
813 in activity and thermal stability. *Photosynthesis Res.* 124, 191-198.

814 Hertle, A.P., Blunder, T., Wunder, T., Pesaresi, P., Pribil, M., Armbruster, U., and Leister, D. (2013).  
815 PGRL1 Is the Elusive Ferredoxin-Plastoquinone Reductase in Photosynthetic Cyclic Electron Flow.  
816 *Mol. Cell* 49, 511-523.

817 Hirasawa, M., Schurmann, P., Jacquot, J., Manieri, W., Jacquot, P., Keryer, E., Hartman, F., and Knaff,  
818 D. (1999). Oxidation-reduction properties of chloroplast thioredoxins, Ferredoxin : Thioredoxin  
819 reductase, and thioredoxin f-regulated enzymes. *Biochemistry (N. Y. )* 38, 5200-5205.

820 Horvath, E., Peter, S., Joet, T., Rumeau, D., Cournac, L., Horvath, G., Kavanagh, T., Schafer, C.,  
821 Peltier, G., and Medgyesy, P. (2000). Targeted inactivation of the plastid *ndhB* gene in tobacco results  
822 in an enhanced sensitivity of photosynthesis to moderate stomatal closure. *Plant Physiol.* 123, 1337-  
823 1349.

824 Johnson, G.N. (2011). Physiology of PSI cyclic electron transport in higher plants. 1807, 384-389,  
825 doi/<https://doi.org/10.1016/j.bbabi.2010.11.009>.

826 Joliot, P. and Joliot, A. (2002). Cyclic electron transfer in plant leaf. *Proc. Natl. Acad. Sci. U. S. A.* 99,  
827 10209-10214.

828 Joliot, P. and Johnson, G.N. (2011). Regulation of cyclic and linear electron flow in higher plants. *Proc.*  
829 *Natl. Acad. Sci. U. S. A.* 108, 13317-13322.

830 Junesch, U. and Gräber, P. (1991). The Rate of ATP-Synthesis as a Function of Delta-pH and Delta-Psi  
831 Catalyzed by the Active, Reduced H<sup>+</sup>-Atpase from Chloroplasts. *FEBS Lett.* 294, 275-278.

832 Kanazawa, A., Ostendorf, E., Kohzuma, K., Hoh, D., Strand, D.D., Sato-Cruz, M., Savage, L., Cruz,  
833 J.A., Fisher, N., Froehlich, J.E., and Kramer, D.M. (2017). Chloroplast ATP Synthase Modulation of  
834 the Thylakoid Proton Motive Force: Implications for Photosystem I and Photosystem II  
835 Photoprotection. *Front. Plant Sci.* 8, 719.

836 Kirchsteiger, K., Pulido, P., Gonzalez, M., and Javier Cejudo, F. (2009). NADPH Thioredoxin  
837 Reductase C Controls the Redox Status of Chloroplast 2-Cys Peroxiredoxins in *Arabidopsis thaliana*.  
838 *Mol. Plant.* 2, 298-307.

839 Klughammer, C., Siebke, K., and Schreiber, U. (2013). Continuous ECS-indicated recording of the  
840 proton-motive charge flux in leaves. *Photosynthesis Res.* 117, 471-487.

841 Kono, M. and Terashima, I. (2014). Long-term and short-term responses of the photosynthetic electron  
842 transport to fluctuating light. *J. Photochem. Photobiol. B.* 137, 89-99.

843 Kou, J., Takahashi, S., Fan, D., Badger, M.R., and Chow, W.S. (2015). Partially dissecting the steady-  
844 state electron fluxes in Photosystem I in wild-type and *pgr5* and *ndh* mutants of *Arabidopsis*. *Front.*  
845 *Plant Sci.* 6, 758.

846 Kramer, D.M. and Crofts, A.R. (1989). Activation of the Chloroplast ATPase Measured by the  
847 Electrochromic Change in Leaves of Intact Plants. *Biochim. Biophys. Acta* 976, 28-41.

848 Kramer, D.M., Johnson, G., Kiirats, O., and Edwards, G.E. (2004). New fluorescence parameters for  
849 the determination of Q(A) redox state and excitation energy fluxes. *Photosynthesis Res.* 79, 209-218.

850 Kramer, D., Wise, R., Frederick, J., Alm, D., Hesketh, J., Ort, D., and Crofts, A. (1990). Regulation of  
851 Coupling Factor in Field-Grown Sunflower - a Redox Model Relating Coupling Factor Activity to the  
852 Activities of Other Thioredoxin-Dependent Chloroplast Enzymes. *Photosynthesis Res.* 26, 213-222.

853 Leister, D. and Shikanai, T. (2013). Complexities and protein complexes in the antimycin A-sensitive  
854 pathway of cyclic electron flow in plants. *Front. Plant Sci.* 4, 161.

- 855 Lepistö, A., Kangasjärvi, S., Luomala, E., Brader, G., Sipari, N., Keränen, M., Keinänen, M., and  
856 Rintamäki, E. (2009). Chloroplast NADPH-Thioredoxin Reductase Interacts with Photoperiodic  
857 Development in Arabidopsis. *Plant Physiol.* 149, 1261-1276.
- 858 Lepistö, A., Pakula, E., Toivola, J., Krieger-Liszkay, A., Vignols, F., and Rintamäki, E. (2013).  
859 Deletion of chloroplast NADPH-dependent thioredoxin reductase results in inability to regulate starch  
860 synthesis and causes stunted growth under short-day photoperiods. *J. Exp. Bot.* 64, 3843-3854.
- 861 Livingston, A.K., Cruz, J.A., Kohzuma, K., Dhingra, A., and Kramer, D.M. (2010). An Arabidopsis  
862 Mutant with High Cyclic Electron Flow around Photosystem I (hcef) Involving the NADPH  
863 Dehydrogenase Complex. *Plant Cell* 22, 221-233.
- 864 Martin, M., Noarbe, D.M., Serrot, P.H., and Sabater, B. (2015). The rise of the photosynthetic rate  
865 when light intensity increases is delayed in *ndh* gene-defective tobacco at high but not at low CO<sub>2</sub>  
866 concentrations. *Front. Plant Sci.* 6, 34.
- 867 Martinsuo, P., Pursiheimo, S., Aro, E., and Rintamäki, E. (2003). Dithiol oxidant and disulfide  
868 reductant dynamically regulate the phosphorylation of light-harvesting complex II proteins in thylakoid  
869 membranes. *Plant Physiol.* 133, 37-46.
- 870 McKinney, D., Buchanan, B., and Wolosiuk, R. (1978). Activation of Chloroplast ATPase by Reduced  
871 Thioredoxin. *Phytochemistry* 17, 794-795.
- 872 Miyake, C., Shinzaki, Y., Miyata, M., and Tomizawa, K. (2004). Enhancement of cyclic electron flow  
873 around PSI at high light and its contribution to the induction of non-photochemical quenching of chl  
874 fluorescence in intact leaves of tobacco plants. *Plant Cell Physiol* 45, 1426-1433.

875 Munekage, Y., Hojo, M., Meurer, J., Endo, T., Tasaka, M., and Shikanai, T. (2002). PGR5 is involved  
876 in cyclic electron flow around photosystem I and is essential for photoprotection in Arabidopsis. *Cell*  
877 110, 361-371.

878 Munekage, Y., Hashimoto, M., Miyake, C., Tomizawa, K., Endo, T., Tasaka, M., and Shikanai, T.  
879 (2004). Cyclic electron flow around photosystem I is essential for photosynthesis. *Nature* 429, 579-582.

880 Murashige, T. and Skoog, F. (1962). A Revised Medium for Rapid Growth and Bio Assays with  
881 Tobacco Tissue Cultures. *Physiol. Plantarum* 15, 473-497.

882 Nalin, C. and McCarty, R. (1984). Role of a Disulfide Bond in the Gamma-Subunit in Activation of the  
883 Atpase of Chloroplast Coupling Factor-i. *J. Biol. Chem.* 259, 7275-7280.

884 Naranjo, B., Mignee, C., Krieger-Liszkay, A., Hornero-Mendez, D., Gallardo-Guerrero, L., Javier  
885 Cejudo, F., and Lindahl, M. (2016). The chloroplast NADPH thioredoxin reductase C, NTRC, controls  
886 non-photochemical quenching of light energy and photosynthetic electron transport in Arabidopsis.  
887 *Plant Cell Environ.* 39, 804-822.

888 Nikkanen, L. and Rintamäki, E. (2014). Thioredoxin-dependent regulatory networks in chloroplasts  
889 under fluctuating light conditions. *Philos. Trans. R. Soc. B-Biol. Sci.* 369, 20130224.

890 Nikkanen, L., Toivola, J., and Rintamäki, E. (2016). Crosstalk between chloroplast thioredoxin systems  
891 in regulation of photosynthesis. *Plant Cell Environ.* 39, 1691-1705.

892 Niyogi, K.K. and Truong, T.B. (2013). Evolution of flexible non-photochemical quenching  
893 mechanisms that regulate light harvesting in oxygenic photosynthesis. *Curr. Opin. Plant Biol.* 16, 307-  
894 314, doi/<https://doi.org/10.1016/j.pbi.2013.03.011>.

895 Okegawa, Y., Kagawa, Y., Kobayashi, Y., and Shikanai, T. (2008). Characterization of factors  
896 affecting the activity of photosystem I cyclic electron transport in chloroplasts. *Plant Cell Physiol* 49,  
897 825-834.

898 Peltier, G., Aro, E., and Shikanai, T. (2016). NDH-1 and NDH-2 Plastoquinone Reductases in  
899 Oxygenic Photosynthesis. *Annual Review of Plant Biology, Annu. Rev. Plant Biol.* 67, 55-80.

900 Perez-Ruiz, J.M., Spinola, M.C., Kirchsteiger, K., Moreno, J., Sahrawy, M., and Cejudo, F.J. (2006).  
901 Rice NTRC is a high-efficiency redox system for chloroplast protection against oxidative damage.  
902 *Plant Cell* 18, 2356-2368.

903 Pérez-Ruiz, J.M., Naranjo, B., Ojeda, V., Guinea, M., and Cejudo, F.J. (2017). NTRC-dependent redox  
904 balance of 2-Cys peroxiredoxins is needed for optimal function of the photosynthetic apparatus. *Proc.*  
905 *Natl. Acad. Sci. U. S. A.* 114, 12069-12074.

906 Petroutsos, D., Terauchi, A.M., Busch, A., Hirschmann, I., Merchant, S.S., Finazzi, G., and Hippler, M.  
907 (2009). PGRL1 Participates in Iron-induced Remodeling of the Photosynthetic Apparatus and in  
908 Energy Metabolism in *Chlamydomonas reinhardtii*. *J. Biol. Chem.* 284, 32770-32781.

909 Porra, R., Thompson, W., and Kriedemann, P. (1989). Determination of Accurate Extinction  
910 Coefficients and Simultaneous-Equations for Assaying Chlorophyll-a and Chlorophyll-B Extracted  
911 with 4 Different Solvents - Verification of the Concentration of Chlorophyll Standards by Atomic-  
912 Absorption Spectroscopy. *Biochim. Biophys. Acta* 975, 384-394.

913 Pulido, P., Spinola, M.C., Kirchsteiger, K., Guinea, M., Belen Pascual, M., Sahrawy, M., Sandalio,  
914 L.M., Dietz, K., Gonzalez, M., and Cejudo, F.J. (2010). Functional analysis of the pathways for 2-Cys  
915 peroxiredoxin reduction in *Arabidopsis thaliana* chloroplasts. *J. Exp. Bot.* 61, 4043-4054.

916 Rintamäki, E., Salonen, M., Suoranta, U., Carlberg, I., Andersson, B., and Aro, E. (1997).  
917 Phosphorylation of light-harvesting complex II and photosystem II core proteins shows different  
918 irradiance-dependent regulation in vivo - Application of phosphothreonine antibodies to analysis of  
919 thylakoid phosphoproteins. *J. Biol. Chem.* 272, 30476-30482.

920 Rintamäki, E., Martinsuo, P., Pursiheimo, S., and Aro, E. (2000). Cooperative regulation of light-  
921 harvesting complex II phosphorylation via the plastoquinol and ferredoxin-thioredoxin system in  
922 chloroplasts. *Proc. Natl. Acad. Sci. U. S. A.* 97, 11644-11649.

923 Rochaix, J. (2011). Regulation of photosynthetic electron transport. *Biochim. Biophys. Acta-Bioenerg.*  
924 1807, 375-383.

925 Ruban, A.V. (2016). Nonphotochemical Chlorophyll Fluorescence Quenching: Mechanism and  
926 Effectiveness in Protecting Plants from Photodamage. *Plant Physiol.* 170, 1903-1916.

927 Ruban, A.V. and Johnson, M.P. (2009). Dynamics of higher plant photosystem cross-section associated  
928 with state transitions. *Photosynthesis Res.* 99, 173-183.

929 Rumeau, D., Becuwe-Linka, N., Beyly, A., Louwagie, M., Garin, J., and Peltier, G. (2005). New  
930 subunits NDH-M, -N, and -O, encoded by nuclear genes, are essential for plastid Ndh complex  
931 functioning in higher plants. *Plant Cell* 17, 219-232.

932 Schneider, C.A., Rasband, W.S., and Eliceiri, K.W. (2012). NIH Image to ImageJ: 25 years of image  
933 analysis. 9, 671-675.

934 Schreiber, U. and Klughammer, C. (2008). New accessory for the DUAL-PAM-100: The P515/535  
935 module and examples of its application. PAM Application Notes 1, 1-10.

936 Schürmann, P. and Buchanan, B.B. (2008). The ferredoxin/thioredoxin system of oxygenic  
937 photosynthesis. Antioxid. Redox Signal. 10, 1235-1273.

938 Serrato, A.J., Perez-Ruiz, J.M., Spinola, M.C., and Cejudo, F.J. (2004). A novel NADPH thioredoxin  
939 reductase, localized in the chloroplast, which deficiency causes hypersensitivity to abiotic stress in  
940 *Arabidopsis thaliana*. J. Biol. Chem. 279, 43821-43827.

941 Shapiguzov, A., Chai, X., Fucile, G., Longoni, P., Zhang, L., and Rochaix, J.-. (2016). Activation of  
942 the Stt7/STN7 Kinase through Dynamic Interactions with the Cytochrome b(6)f Complex (vol 171, pg  
943 82, 2016). Plant Physiol. 171, 1533-1533.

944 Shikanai, T., Endo, T., Hashimoto, T., Yamada, Y., Asada, K., and Yokota, A. (1998). Directed  
945 disruption of the tobacco *ndhB* gene impairs cyclic electron flow around photosystem I. Proc. Natl.  
946 Acad. Sci. U. S. A. 95, 9705-9709.

947 Shikanai, T. (2016). Chloroplast NDH: A different enzyme with a structure similar to that of  
948 respiratory NADH dehydrogenase. Biochim. Biophys. Acta-Bioenerg. 1857, 1015-1022.

949 Shikanai, T. and Yamamoto, H. (2017). Contribution of Cyclic and Pseudo-cyclic Electron Transport to  
950 the Formation of Proton Motive Force in Chloroplasts. Mol. Plant. 10, 20-29.

951 Sievers, F., Wilm, A., Dineen, D., Gibson, T.J., Karplus, K., Li, W., Lopez, R., McWilliam, H.,  
952 Remmert, M., Soeding, J., Thompson, J.D., and Higgins, D.G. (2011). Fast, scalable generation of  
953 high-quality protein multiple sequence alignments using Clustal Omega. 7, 539.

954 Stirbet, A., Riznichenko, G.Y., Rubin, A.B., and Govindjee (2014). Modeling chlorophyll a  
955 fluorescence transient: relation to photosynthesis. *Biochemistry (Mosc)* 79, 291-323.

956 Strand, D.D., Fisher, N., and Kramer, D.M. (2017a). The higher plant plastid NAD(P)H  
957 dehydrogenase-like complex (NDH) is a high efficiency proton pump that increases ATP production by  
958 cyclic electron flow. *J. Biol. Chem.* 292, 11850-11860.

959 Strand, D.D., Livingston, A.K., Satoh-Cruz, M., Froehlich, J.E., Maurino, V.G., and Kramer, D.M.  
960 (2015). Activation of cyclic electron flow by hydrogen peroxide in vivo. *Proc. Natl. Acad. Sci. U. S. A.*  
961 112, 5539-5544.

962 Strand, D.D., Fisher, N., Davis, G.A., and Kramer, D.M. (2016a). Redox regulation of the antimycin A  
963 sensitive pathway of cyclic electron flow around photosystem I in higher plant thylakoids. *Biochim.*  
964 *Biophys. Acta-Bioenerg.* 1857, 1-6.

965 Strand, D.D., Fisher, N., and Kramer, D.M. (2016b). Distinct Energetics and Regulatory Functions of  
966 the Two Major Cyclic Electron Flow Pathways in Chloroplasts In *Chloroplasts: Current Research and*  
967 *Future Trends*, Kirchhoff, H., ed (WYMONDHAM; 32 HEWITTS LANE, WYMONDHAM NR 18  
968 0JA, ENGLAND: CAISTER ACADEMIC PRESS) pp. 89-100.

969 Strand, D.D., Livingston, A.K., Satoh-Cruz, M., Koepke, T., Enlow, H.M., Fisher, N., Froehlich, J.E.,  
970 Cruz, J.A., Minhas, D., Hixson, K.K., Kohzuma, K., Lipton, M., Dhingra, A., and Kramer, D.M.

- 971 (2017b). Defects in the Expression of Chloroplast Proteins Leads to H<sub>2</sub>O<sub>2</sub> Accumulation and
- 972 Activation of Cyclic Electron Flow around Photosystem I. *Front. Plant Sci.* 7, 2073.
- 973 Suorsa, M., Jarvi, S., Grieco, M., Nurmi, M., Pietrzykowska, M., Rantala, M., Kangasjarvi, S.,
- 974 Paakkarinen, V., Tikkanen, M., Jansson, S., and Aro, E. (2012). PROTON GRADIENT
- 975 REGULATION5 Is Essential for Proper Acclimation of Arabidopsis Photosystem I to Naturally and
- 976 Artificially Fluctuating Light Conditions. *Plant Cell* 24, 2934-2948.
- 977 Suorsa, M., Grieco, M., Järvi, S., Gollan, P.J., Kangasjärvi, S., Tikkanen, M., and Aro, E. (2013).
- 978 PGR5 ensures photosynthetic control to safeguard photosystem I under fluctuating light conditions.
- 979 *Plant Signal Behav* 8, e22714.
- 980 Suorsa, M. (2015). Cyclic electron flow provides acclimatory plasticity for the photosynthetic
- 981 machinery under various environmental conditions and developmental stages. *Front. Plant Sci.* 6, 800.
- 982 Suorsa, M., Rossi, F., Tadini, L., Labs, M., Colombo, M., Jahns, P., Kater, M.M., Leister, D., Finazzi,
- 983 G., Aro, E., Barbato, R., and Pesaresi, P. (2016). PGR5-PGRL1-Dependent Cyclic Electron Transport
- 984 Modulates Linear Electron Transport Rate in *Arabidopsis thaliana*. *Mol. Plant.* 9, 271-288.
- 985 Thormählen, I., Meitzel, T., Groysman, J., Ochsner, A.B., von Roepenack-Lahaye, E., Naranjo, B.,
- 986 Cejudo, F.J., and Geigenberger, P. (2015). Thioredoxin f1 and NADPH-dependent thioredoxin
- 987 reductase C have overlapping functions in regulating photosynthetic metabolism and plant growth in
- 988 response to varying light conditions. *Plant Physiol.* 169, 1766-1786.
- 989 Thormählen, I., Zupok, A., Rescher, J., Leger, J., Weissenberger, S., Groysman, J., Orwat, A., Chatel-
- 990 Innocenti, G., Issakidis-Bourguet, E., Armbruster, U., and Geigenberger, P. (2017). Thioredoxins Play

991 a Crucial Role in Dynamic Acclimation of Photosynthesis in Fluctuating Light. *Mol. Plant.* 10, 168-  
992 182.

993 Tikkanen, M. and Aro, E.M. (2014). Integrative regulatory network of plant thylakoid energy  
994 transduction. *Trends Plant Sci.* 19, 10-17.

995 Tikkanen, M., Pippo, M., Suorsa, M., Sirpio, S., Mulo, P., Vainonen, J., Vener, A., Allahverdiyeva, Y.,  
996 and Aro, E.M. (2006). State transitions revisited - a buffering system for dynamic low light acclimation  
997 of Arabidopsis. *Plant Mol. Biol.* 62, 779-793.

998 Tikkanen, M., Grieco, M., Kangasjarvi, S., and Aro, E. (2010). Thylakoid Protein Phosphorylation in  
999 Higher Plant Chloroplasts Optimizes Electron Transfer under Fluctuating Light. *Plant Physiol.* 152,  
1000 723-735.

1001 Tikkanen, M., Grieco, M., Nurmi, M., Rantala, M., Suorsa, M., and Aro, E. (2012). Regulation of the  
1002 photosynthetic apparatus under fluctuating growth light. 367, 3486-3493.

1003 Tikkanen, M., Rantala, S., and Aro, E. (2015). Electron flow from PSII to PSI under high light is  
1004 controlled by PGR5 but not by PSBS. *Front. Plant Sci.* 6, 521.

1005 Tiwari, A., Mamedov, F., Grieco, M., Suorsa, M., Jajoo, A., Styring, S., Tikkanen, M., and Aro, E.  
1006 (2016). Photodamage of iron-sulphur clusters in photosystem I induces non-photochemical energy  
1007 dissipation. *Nat. Plants* 2, 16035.

1008 Toivola, J., Nikkanen, L., Dahlström, K.M., Salminen, T.A., Lepistö, A., Vignols, F., and Rintamäki,  
1009 E. (2013). Overexpression of chloroplast NADPH-dependent thioredoxin reductase in Arabidopsis

enhances leaf growth and elucidates in vivo function of reductase and thioredoxin domains. *Front. Plant Sci.* 4, 389.

Toth, S.Z., Schansker, G., and Strasser, R.J. (2007). A non-invasive assay of the plastoquinone pool redox state based on the OJIP-transient. *Photosynthesis Res.* 93, 193-203.

Townsend, A.J., Ware, M.A., and Ruban, A.V. (2017). Dynamic interplay between photodamage and photoprotection in photosystem II. *Plant. Cell. Environ.*

Trotta, A., Suorsa, M., Rantala, M., Lundin, B., and Aro, E. (2016). Serine and threonine residues of plant STN7 kinase are differentially phosphorylated upon changing light conditions and specifically influence the activity and stability of the kinase. *Plant J.* 87, 484-494.

Vener, A., VanKan, P., Rich, P., Ohad, I., and Andersson, B. (1997). Plastoquinol at the quinol oxidation site of reduced cytochrome bf mediates signal transduction between light and protein phosphorylation: Thylakoid protein kinase deactivation by a single-turnover flash. *Proc. Natl. Acad. Sci. U. S. A.* 94, 1585-1590.

Walter, M., Chaban, C., Schutze, K., Batistic, O., Weckermann, K., Nake, C., Blazevic, D., Grefen, C., Schumacher, K., Oecking, C., Harter, K., and Kudla, J. (2004). Visualization of protein interactions in living plant cells using bimolecular fluorescence complementation. *Plant J.* 40, 428-438.

Wang, C., Yamamoto, H., and Shikanai, T. (2015). Role of cyclic electron transport around photosystem I in regulating proton motive force. *Biochim. Biophys. Acta-Bioenerg.* 1847, 931-938.

- 1028 Wang, P., Liu, J., Liu, B., Da, Q., Feng, D., Su, J., Zhang, Y., Wang, J., and Wang, H. (2014).
- 1029 Ferredoxin: Thioredoxin Reductase Is Required for Proper Chloroplast Development and Is Involved in
- 1030 the Regulation of Plastid Gene Expression in *Arabidopsis thaliana*. *Mol. Plant.* 7, 1586-1590.
- 1031 Yamamoto, H., Peng, L., Fukao, Y., and Shikanai, T. (2011). An Src Homology 3 Domain-Like Fold
- 1032 Protein Forms a Ferredoxin Binding Site for the Chloroplast NADH Dehydrogenase-Like Complex in
- 1033 *Arabidopsis*. *Plant Cell* 23, 1480-1493.
- 1034 Yamamoto, H. and Shikanai, T. (2013). In Planta Mutagenesis of Src Homology 3 Domain-like Fold of
- 1035 NdhS, a Ferredoxin-binding Subunit of the Chloroplast NADH Dehydrogenase-like Complex in
- 1036 *Arabidopsis* A conserved Arg-193 plays a critical role in ferredoxin binding. *J. Biol. Chem.* 288, 36328-
- 1037 36337.
- 1038 Yamori, W., Sakata, N., Suzuki, Y., Shikanai, T., and Makino, A. (2011). Cyclic electron flow around
- 1039 photosystem I via chloroplast NAD(P)H dehydrogenase (NDH) complex performs a significant
- 1040 physiological role during photosynthesis and plant growth at low temperature in rice. *Plant J.* 68, 966-
- 1041 976.
- 1042 Yamori, W., Shikanai, T., and Makino, A. (2015). Photosystem I cyclic electron flow via chloroplast
- 1043 NADH dehydrogenase-like complex performs a physiological role for photosynthesis at low light (vol
- 1044 5, 13908, 2015). *Sci. Rep.* 5, 15593.
- 1045 Yamori, W., Makino, A., and Shikanai, T. (2016). A physiological role of cyclic electron transport
- 1046 around photosystem I in sustaining photosynthesis under fluctuating light in rice. *Sci. Rep.* 6, 20147.

1047 Yamori, W. and Shikanai, T. (2016). Physiological Functions of Cyclic Electron Transport Around  
1048 Photosystem I in Sustaining Photosynthesis and Plant Growth. *Annu. Rev. Plant Biol.* 67, 81-106.

1049 Yoshida, K., Hara, S., and Hisabori, T. (2015). Thioredoxin Selectivity for Thiol-Based Redox  
1050 Regulation of Target Proteins in Chloroplasts. *J. Biol. Chem.* 290, 19540.

1051 Yoshida, K. and Hisabori, T. (2016). Two distinct redox cascades cooperatively regulate chloroplast  
1052 functions and sustain plant viability. *Proc. Natl. Acad. Sci. U. S. A.* 113, E3967-E3976.

1053 Yoshida, K. and Hisabori, T. (2017). Distinct Electron Transfer from Ferredoxin-Thioredoxin  
1054 Reductase to Multiple Thioredoxin Isoforms in Chloroplasts. *Biochem. J.* 474, 1347-1360,  
1055 doi/10.1042/BCJ20161089.

1056 Zaffagnini, M., De Mia, M., Morisse, S., Di Giacinto, N., Marchand, C.H., Maes, A., Lemaire, S.D.,  
1057 and Trost, P. (2016). Protein S-nitrosylation in photosynthetic organisms: A comprehensive overview  
1058 with future perspectives. *Biochim. Biophys. Acta-Proteom.* 1864, 952-966.

1059

1060

1061

1062

1063

1064

1065

1066

1067

1068

# FIGURE LEGENDS

**Figure 1.** *In vivo* redox state of NTRC in dark-adapted and illuminated leaves.

(A) and (B) Total protein extract was isolated from WT (A) and OE-NTRC (B) leaves incubated in darkness (D), or illuminated for 2h in low light (LL, 40  $\mu\text{mol photons m}^{-2} \text{s}^{-1}$ ), growth light (GL, 200  $\mu\text{mol photons m}^{-2} \text{s}^{-1}$ ) or high light (HL, 800  $\mu\text{mol photons m}^{-2} \text{s}^{-1}$ ). Free thiols of proteins were blocked with NEM, disulfides reduced with DTT and newly formed thiols alkylated with MAL-PEG. The *in vivo*-reduced form of NTRC therefore migrates faster in SDS-PAGE than the *in vivo* oxidized forms. –DTT stands for the unlabeled control sample where DTT was not added after incubating the leaf extracts in a buffer containing NEM. Protein content of samples has only been equalized based on the amount of starting leaf material, and the apparent differences in band intensity should not be taken as indication of differences in NTRC content between light treatments. For an analysis of the origin of different MAL-PEG labelled bands see Suppl. Fig. 1.

(C) NTRC redox state in WT during a transition from dark to growth light. Samples were taken from darkness (2h) (D) and 15, 30, 45 and 60 seconds after onset of illumination.

**Figure 2.** Post-illumination fluorescence rise (PIFR) in dark-adapted leaves.

(A) and (B) PIFR was measured from WT, OE-NTRC, *ntrc* (A), *pgr5* and *ndho* (B) leaves. The smaller windows show magnifications of the ~100 s of the PIFR. The cyan bars indicate exposure to a 480 nm measuring light of 0.28  $\mu\text{mol photons m}^{-2} \text{s}^{-1}$ , the white bar depicts illumination with 67  $\mu\text{mol photons m}^{-2} \text{s}^{-1}$  white light and the red bar shows the duration of a pulse of far red light. The dashed lines indicate the  $F_0$  values of the lines. The curves are averages from 3–7 measurements of individual leaves.

(C) PIFR in WT and OE-NTRC *ndho*. Only the post-illumination phase of the experiment is shown in the figure. The curves are averages from 3–4 measurements of individual leaves.

1096 **Figure 3.** Redox state of the PQ pool in dark-adapted leaves.

1097 (A–F) PQ pool redox state in darkness was determined from measurement of the OJIP transients in  
1098 dark-adapted leaves (black) and leaves pre-illuminated with far red light (red). Data is presented as  
1099 averaged curves from 5–10 individual measurements on a logarithmic time scale from WT (A), OE-  
1100 NTRC (B), *ntrc* (C), *pgr5* (D), *ndho* (E) and OE-NTRC *ndho* (F).

1101 (G) Proportions of reduced  $Q_A$  calculated as  $(F_J - F_{J_{ox}}) / (F_m - F_{J_{ox}})$ . Values are averages from 5–10  
1102 measurements from individual leaves  $\pm$  SE. \* indicates statistically significant difference to WT  
1103 according to Student's T test ( $P < 0.05$ ). All values are normalized to dark-adapted  $F_m$ .

1104 (H) Determination of phosphorylation status of LHCII proteins in WT, *ntrc*, OE-NTRC and *stn7* after 2  
1105 h of darkness and in low light ( $40 \mu\text{mol photons m}^{-2} \text{s}^{-1}$ ), growth light ( $200 \mu\text{mol photons m}^{-2} \text{s}^{-1}$ ) and  
1106 high light ( $600 \mu\text{mol photons m}^{-2} \text{s}^{-1}$ ).  $0.4 \mu\text{g}$  of thylakoid extracts were separated with SDS-PAGE and  
1107 detected with a Phosphothreonine-specific antibody. Coomassie Brilliant Blue staining of LHCII on the  
1108 membrane (CBB-LHCII) was used as loading control.

1109

1110 **Figure 4.** Content of proteins functioning in the photosynthetic electron transfer chain (PETC), cyclic  
1111 electron flow (CEF) and chlororespiration in WT, *ntrc*, OE-NTRC, *pgr5* and *ndho*.

1112 (A) Representative immunoblots showing the content of D1, PsaB, Cyt *f*, NdhH, NdhS, PGR5, PGRL1  
1113 and PTOX. Appropriate amount of thylakoid extract was separated with SDS-PAGE and probed with  
1114 specific antibodies.

1115 (B) Averages of quantified protein content  $\pm$ SE in 3–5 biological replicates. Statistically significant  
1116 differences to WT according to Student's T-tests ( $P < 0.05$ ) are marked with \*. Equal loading was  
1117 confirmed by and protein quantification normalized according to staining with Li-Cor Revert Total  
1118 Protein Stain.

1119

1120

1121

1122

1123

**Figure 5.** Generation of the proton gradient during dark-to-light transitions.

**(A–B)** Proton motive force (*pmf*) at specific time points during transitions from dark to 166  $\mu\text{mol photons m}^{-2} \text{s}^{-1}$  actinic light (AL) in dark-adapted leaves of WT Col-0, OE-NTRC, *ntrc*, *ndho* and OE-NTRC *ndho* (A) and in WT Col-*gll*, OE-NTRC, *pgr5* and OE-NTRC *pgr5* (B). The *pmf* was measured as light-induced change in the ECS signal ( $\text{ECS}_T$ ) and normalized with the magnitude of ECS induced by a 20  $\mu\text{s}$  saturating single turnover flash administered prior to the onset of AL ( $\text{ECS}_{ST}$ ). The small window in the bottom left corner of (A) shows representative P700 oxidation kinetics measured with the Dual-PAM spectrometer in synchronization with the ECS data. Saturating pulses were administered with 15 s intervals during the P700 measurement. Values are averages from 4–16 individual measurements  $\pm\text{SE}$ .

**(C–D)** Conductivity of the thylakoid membrane to protons ( $g_{H^+}$ ), calculated as the inverse of the time constant of a first order fit to the decay of ECS during 250 ms dark intervals.

**(E)** Total *pmf* and its partitioning to  $\Delta\text{pH}$  and  $\Delta\Psi$  after 3 min illumination with low, growth or high light.

**(F)** Data in (E) represented as percentages of total *pmf*. Values are averages from 4–16 individual measurements  $\pm\text{SE}$ , and statistically significant differences to WT according to Student's T-tests ( $P<0.05$ ) are marked with \*.

**(G)** Mobility shift assays with MAL-PEG labelled protein extracts to determine the *in vivo* redox state of  $\text{CF}_1\gamma$  during first 60 seconds of dark-to-growth light transitions. \* marks an unspecific band of unknown origin.

**Figure 6.** Photosynthetic parameters during dark-to-light transitions.

**(A–E)** Induction of non-photochemical quenching (A), photosystem II quantum yield (B), redox state of the PQ pool ( $1-q_L$ ) (C), P700 oxidation ( $Y(\text{ND})$ ) (D) and PSI acceptor side limitation ( $Y(\text{NA})$ ) (E) were calculated from Chl a fluorescence and 870–820 nm absorbance changes during transitions from dark to 166  $\mu\text{mol photons m}^{-2} \text{s}^{-1}$  actinic light in dark-adapted WT Col-0, *ntrc*, OE-NTRC, *ndho*, OE-NTRC *ndho*, WT Col-*gll*, *pgr5* and OE-NTRC *pgr5* leaves. The graphs are averages from 4–9 individual measurements  $\pm\text{SE}$ .

**Figure 7.** Formation and regulation the proton motive force during changes in light conditions.

**(A–B)** The *pmf* (A) and proton conductivity of the thylakoid membrane( $g_{H^+}$ ) (B) at specific time points during transitions from darkness to low actinic light ( $39 \mu\text{mol photons m}^{-2} \text{s}^{-1}$ ) and from low to high light ( $825 \mu\text{mol photons m}^{-2} \text{s}^{-1}$ ) in dark-adapted leaves of WT Col-0, OE-NTRC, *ntrc*, *ndho* and OE-NTRC *ndho*. The *pmf* and  $g_{H^+}$  were measured and calculated as explained in the legend for Figure 5. The graphs shown are averages from 4–13 individual measurements  $\pm$ SE.

**(C–D)** The *pmf* and  $g_{H^+}$  in dark-adapted leaves of WT Col-*gll*, OE-NTRC, *pgr5* and OE-NTRC *pgr5*. The graphs shown are averages from 3–13 individual measurements  $\pm$ SE.

**Figure 8.** Analysis of Chlorophyll a fluorescence in fluctuating light.

**(A–C)** PSII yield (Y(II) (A), non-photochemical quenching (NPQ) (B) and redox state of the PQ pool (1-qL) (C) in light conditions fluctuating between periods of low actinic light (LL,  $39 \mu\text{mol photons m}^{-2} \text{s}^{-1}$ ) and high light (HL,  $825 \mu\text{mol photons m}^{-2} \text{s}^{-1}$ ) in WT Col-0, OE-NTRC, *ntrc*, *ndho*, OE-NTRC *ndho*, WT Col-*gll*, *pgr5* and OE-NTRC *pgr5*. Five weeks old plants were dark-adapted for 30 min before measuring fluorescence from detached leaves. All values are averages of 3–10 individual measurements  $\pm$ SE.

**Figure 9.** Analysis of P700 oxidation in fluctuating light.

**(A–C)** PSI yield (Y(I) (A), P700 oxidation (Y(ND)) (B) and PSI acceptor side limitation (Y(NA)) (C) in light conditions fluctuating between periods of low actinic light (LL,  $39 \mu\text{mol photons m}^{-2} \text{s}^{-1}$ ) and high light (HL,  $825 \mu\text{mol photons m}^{-2} \text{s}^{-1}$ ) in WT Col-0, OE-NTRC, *ntrc*, *ndho*, OE-NTRC *ndho*, WT Col-*gll*, *pgr5* and OE-NTRC *pgr5*. Five weeks old plants were dark-adapted for 30 min before measuring fluorescence from detached leaves. All values are averages of 3–10 individual measurements  $\pm$ SE.

**Figure 10.** Bimolecular fluorescence complementation (BiFC) tests of *in planta* interactions between chloroplast TRXs and potential CEF target proteins.

The left panel shows yellow fluorescent protein (YFP) fluorescence in green, the middle panel Chlorophyll a autofluorescence in red and the right panel a merged image of YFP, chlorophyll and brightfield images. YFP-N and YFP-C indicate expression of a fusion proteins including the N-terminal and C-terminal parts of YFP, respectively, in tobacco (*Nicotiana benthamiana*) leaves.

**Figure 11.** A schematic model of the role of chloroplast TRX systems in regulating CEF and the *pmf* during dark-to-light transitions and fluctuations in light conditions.

(A–C) Dark-adapted leaves (A), transition from dark to low light (B) and transition from low to high light (C). Blue color indicates the level of reduction, green and red arrows represent the activating and inhibitory effects, respectively, while orange represents the thiol regulation by NTRC and dark yellow by the Fd-TRX system. Thicker lines depict stronger effect than thin and dotted lines. For details see the text.

**TABLES**

**Table 1.** Identification of putative NTRC target proteins in CEF pathways by Co-IP/MS.

Only proteins of which at least two unique peptides were detected, and which were absent from *ntrc* eluates or clearly enriched in WT / OE-NTRC are included. + indicates the presence and – the absence of at least two unique peptides from the protein. MW (kDa) indicates molecular weight, and #Cys the number of conserved cysteine residues (see Suppl. Tables 2–6). For a description of experimental procedures see Materials and methods and for a full list of detected peptides see Suppl. Dataset 1.

AGI code	Description	<i>ntrc</i>	WT	OE-NTRC	MW (kDa)	#Cys
ATCG01110.1	NdhH	-	+	+	45.5	3
AT1G15980.1	Ndh48 (NDF1)	-	+	+	51.0	3
AT4G23890.1	NdhS (CRR31)	-	+	+	27.7	2
AT1G74880.1	NdhO	-	+	+	17.6	0
AT5G21430.2	NdhU	-	+	-	24.3	0
AT2G05620.1	PGR5	-	+	-	14.3	1
ATCG00420.1	NdhJ	+	+	+	18.5	2
AT1G64770.1	Ndh45 (NDF2)	+	+	+	38.0	1

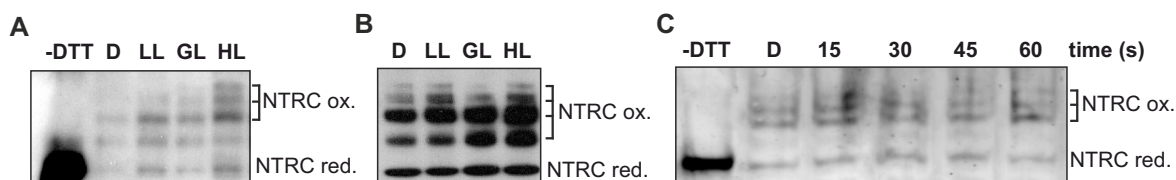


**Figure 1.** *In vivo* redox state of NTRC in dark-adapted and illuminated leaves.

(A) and (B) Total protein extract was isolated from WT (A) and OE-NTRC (B) leaves incubated in darkness (D), or illuminated for 2h in low light (LL,  $40 \mu\text{mol photons m}^{-2} \text{s}^{-1}$ ), growth light (GL,  $200 \mu\text{mol photons m}^{-2} \text{s}^{-1}$ ) or high light (HL,  $800 \mu\text{mol photons m}^{-2} \text{s}^{-1}$ ). Free thiols of proteins were blocked with NEM, disulfides reduced with DTT and newly formed thiols alkylated with MAL-PEG. The *in vivo*-reduced form of NTRC therefore migrates faster in SDS-PAGE than the *in vivo* oxidized forms. -DTT stands for the unlabeled control sample where DTT was not added after incubating the leaf extracts in a buffer containing NEM. Protein content of samples has only been equalized based on the amount of starting leaf material, and the apparent differences in band intensity should not be taken as indication of differences in NTRC content between light treatments. For an analysis of the origin of different MAL-PEG labelled bands see Suppl. Fig. 1.

(C) NTRC redox state in WT during a transition from dark to growth light. Samples were taken from darkness (2h) (D) and 15, 30, 45 and 60 seconds after onset of illumination.

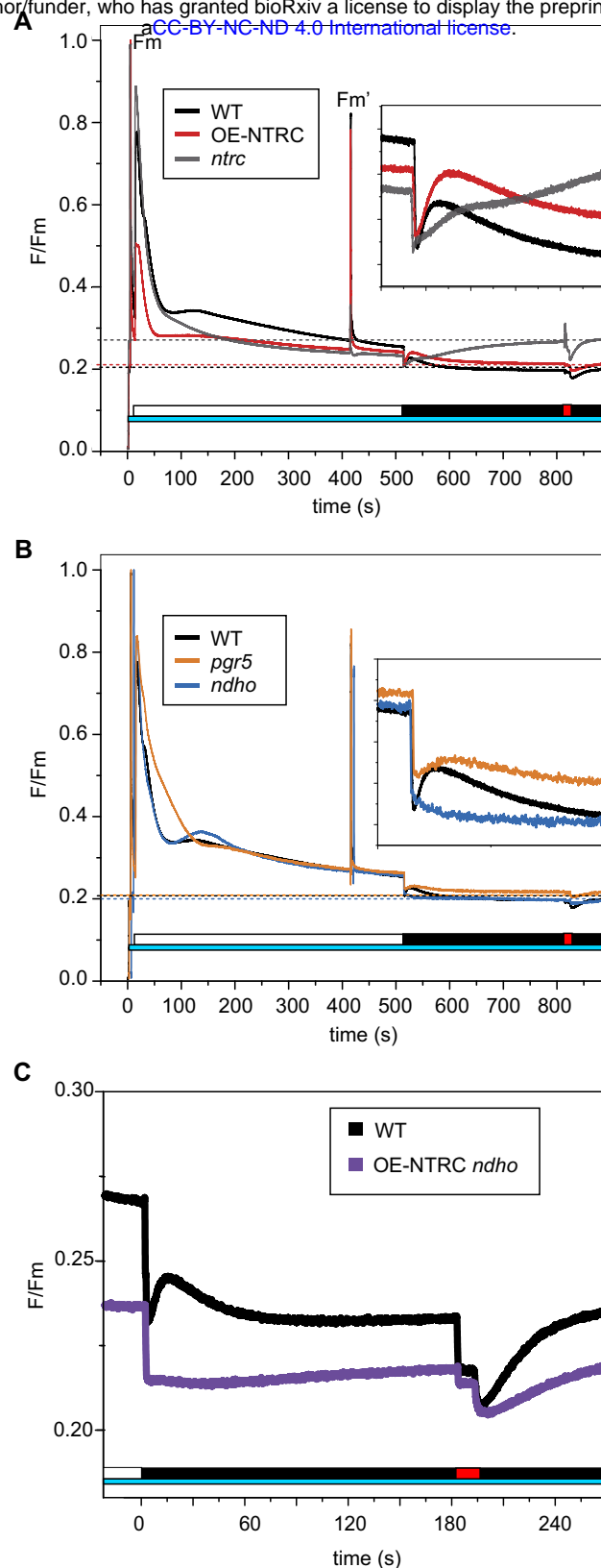


**Figure 2.** Post-illumination fluorescence rise (PIFR) in dark-adapted leaves.

(A) and (B) PIFR was measured from WT, OE-NTRC, *ntrc* (A), *pgr5* and *ndho* (B) leaves. The smaller windows show magnifications of the ~100 s of the PIFR. The cyan bars indicate exposure to a 480 nm measuring light of  $0.28 \mu\text{mol photons m}^{-2} \text{s}^{-1}$ , the white bar depicts illumination with  $67 \mu\text{mol photons m}^{-2} \text{s}^{-1}$  white light and the red bar shows the duration of a pulse of far red light. The dashed lines indicate the  $F_0$  values of the lines. The curves are averages from 3–7 measurements of individual leaves.

(C) PIFR in WT and OE-NTRC *ndho*. Only the post-illumination phase of the experiment is shown in the figure. The curves are averages from 3–4 measurements of individual leaves.

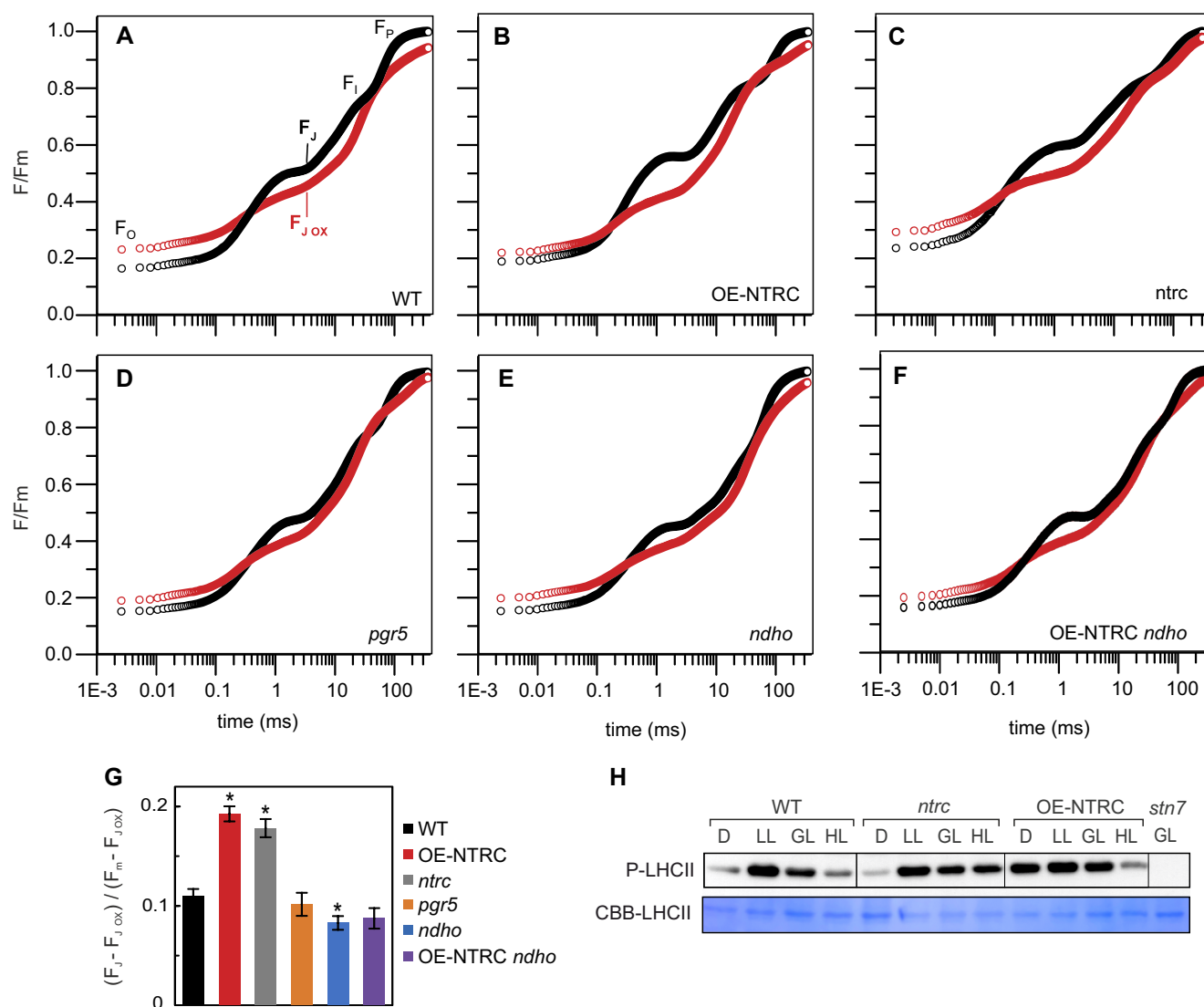


**Figure 3.** Redox state of the PQ pool in dark-adapted leaves.

**(A–F)** PQ pool redox state in darkness was determined from measurement of the OJIP transients in dark-adapted leaves (black) and leaves pre-illuminated with far red light (red). Data is presented as averaged curves from 5–10 individual measurements on a logarithmic time scale from WT (A), OE-NTRC (B), *ntrc* (C), *pgr5* (D), *ndho* (E) and OE-NTRC *ndho* (F).

**(G)** Proportions of reduced  $Q_A$  calculated as  $(F_J - F_{Jox}) / (F_m - F_{Jox})$ . Values are averages from 5–10 measurements from individual leaves  $\pm$  SE. \* indicates statistically significant difference to WT according to Student's T test ( $P < 0.05$ ). All values are normalized to dark-adapted  $F_m$ .

**(H)** Determination of phosphorylation status of LHCII proteins in WT, *ntrc*, OE-NTRC and *stn7* after 2 h of darkness and in low light ( $40 \mu\text{mol photons m}^{-2} \text{s}^{-1}$ ), growth light ( $200 \mu\text{mol photons m}^{-2} \text{s}^{-1}$ ) and high light ( $600 \mu\text{mol photons m}^{-2} \text{s}^{-1}$ ).  $0.4 \mu\text{g}$  of thylakoid extracts were separated with SDS-PAGE and detected with a Phosphothreonine-specific antibody. Coomassie Brilliant Blue staining of LHCII on the membrane (CBB-LHCII) was used as loading control.

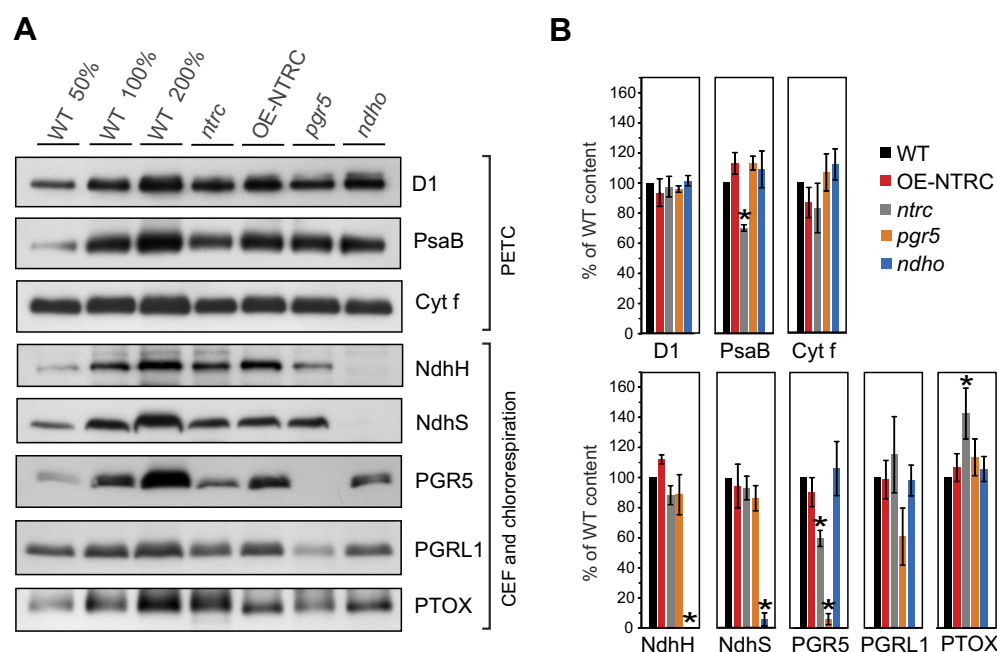


**Figure 4.** Content of proteins functioning in the photosynthetic electron transfer chain (PETC), cyclic electron flow (CEF) and chlororespiration in WT, *ntrc*, OE-NTRC, *pgr5* and *ndho*.

**(A)** Representative immunoblots showing the content of D1, PsaB, Cyt *f*, NdhH, NdhS, PGR5, PGRL1 and PTOX. Appropriate amount of thylakoid extract was separated with SDS-PAGE and probed with specific antibodies.

**(B)** Averages of quantified protein content  $\pm$ SE in 3–5 biological replicates. Statistically significant differences to WT according to Student's T-tests ( $P < 0.05$ ) are marked with \*. Equal loading was confirmed by and protein quantification normalized according to staining with Li-Cor Revert Total Protein Stain.

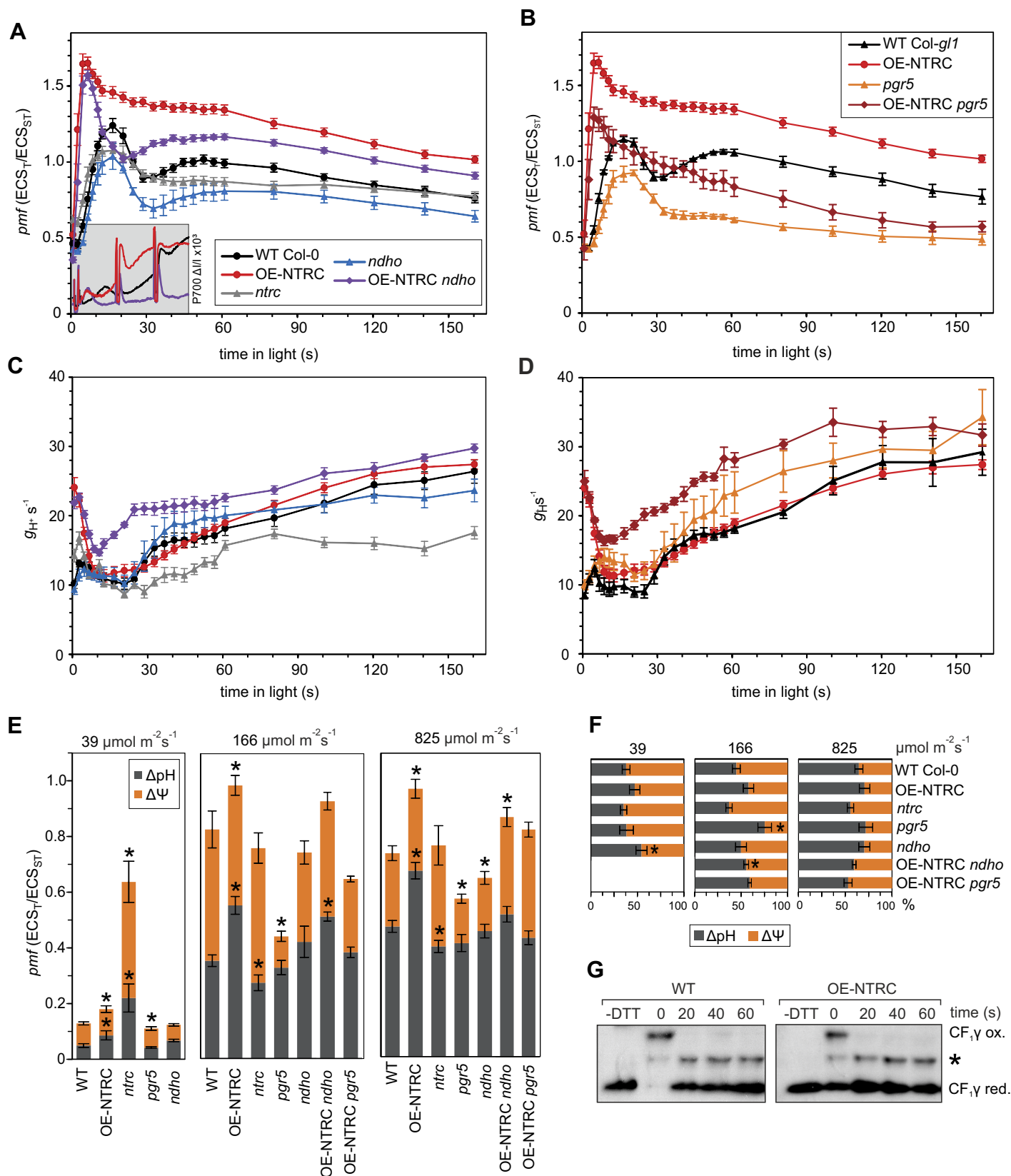


**Figure 5.** Generation of the proton gradient during dark-to-light transitions.

**(A–B)** Proton motive force (*pmf*) at specific time points during transitions from dark to 166  $\mu\text{mol photons m}^{-2} \text{s}^{-1}$  actinic light (AL) in dark-adapted leaves of WT Col-0, OE-NTRC, *ntrc*, *ndho* and OE-NTRC *ndho* (A) and in WT Col-*gl1*, OE-NTRC, *pgr5* and OE-NTRC *pgr5* (B). The *pmf* was measured as light-induced change in the ECS signal ( $\text{ECS}_T$ ) and normalized with the magnitude of ECS induced by a 20  $\mu\text{s}$  saturating single turnover flash administered prior to the onset of AL ( $\text{ECS}_{ST}$ ). The small window in the bottom left corner of (A) shows representative P700 oxidation kinetics measured with the Dual-PAM spectrometer in synchronization with the ECS data. Saturating pulses were administered with 15 s intervals during the P700 measurement. Values are averages from 4–16 individual measurements  $\pm\text{SE}$ .

**(C–D)** Conductivity of the thylakoid membrane to protons ( $g_{H^+}$ ), calculated as the inverse of the time constant of a first order fit to the decay of ECS during 250 ms dark intervals.

**(E)** Total *pmf* and its partitioning to  $\Delta\text{pH}$  and  $\Delta\Psi$  after 3 min illumination with low, growth or high light.

**(F)** Data in (E) represented as percentages of total *pmf*. Values are averages from 4–16 individual measurements  $\pm\text{SE}$ , and statistically significant differences to WT according to Student's T-tests ( $P < 0.05$ ) are marked with \*.

**(G)** Mobility shift assays with MAL-PEG labelled protein extracts to determine the *in vivo* redox state of  $\text{CF}_1\gamma$  during first 60 seconds of dark-to-growth light transitions. \* marks an unspecific band of unknown origin.

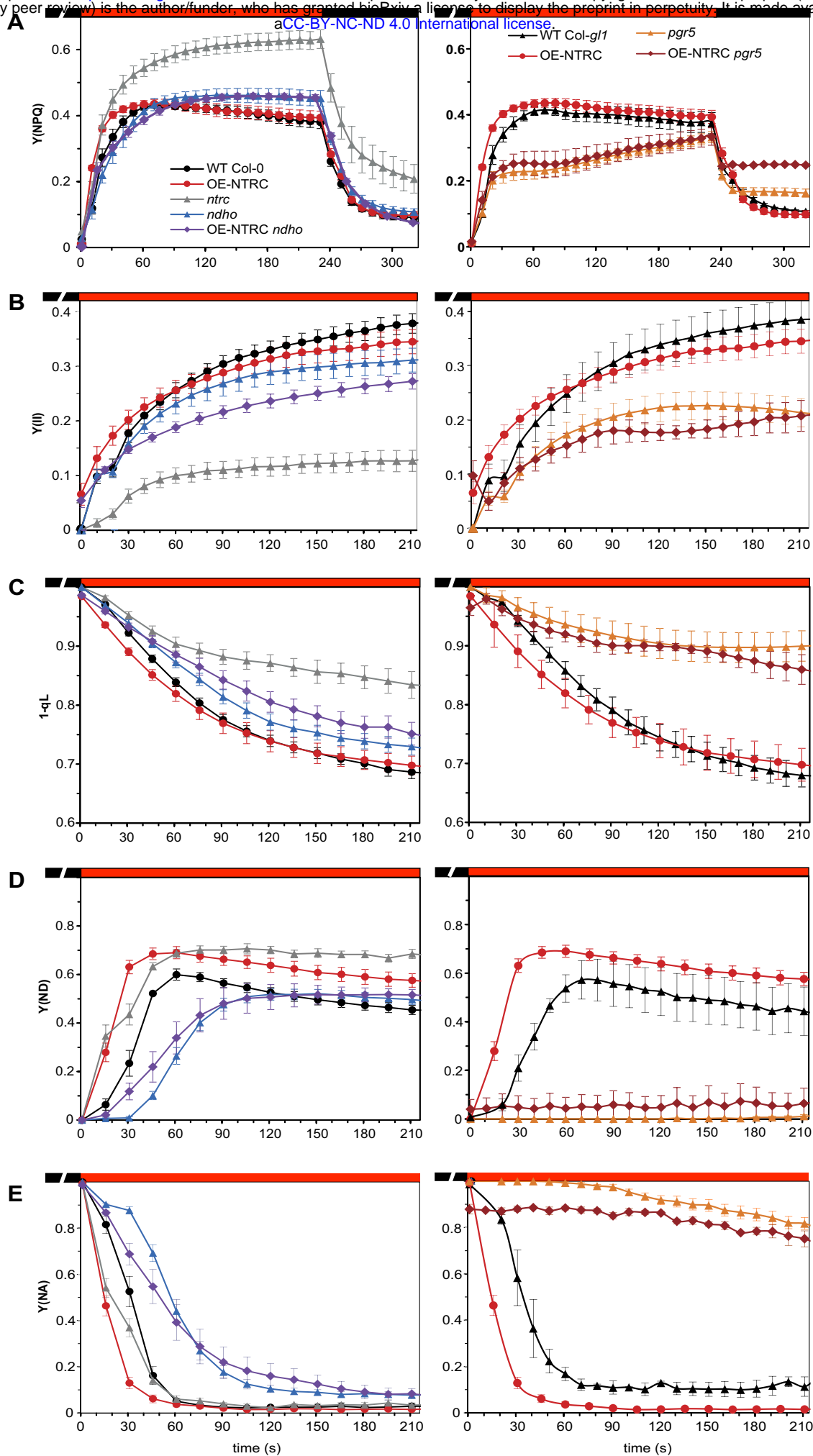


**Figure 6.** Photosynthetic parameters during dark-to-light transitions.

**(A–E)** Induction of non-photochemical quenching (A), photosystem II quantum yield (B), redox state of the PQ pool (1-qL) (C), P700 oxidation (Y(ND)) (D) and PSI acceptor side limitation (Y(NA)) (E) were calculated from Chl a fluorescence and 870–820 nm absorbance changes during transitions from dark to 166  $\mu\text{mol photons m}^{-2} \text{ s}^{-1}$  actinic light in dark-adapted WT Col-0, *ntrc*, OE-NTRC, *ndho*, OE-NTRC *ndho*, WT Col-*gl1*, *pgr5* and OE-NTRC *pgr5* leaves. The graphs are averages from 4–9 individual measurements  $\pm$ SE.

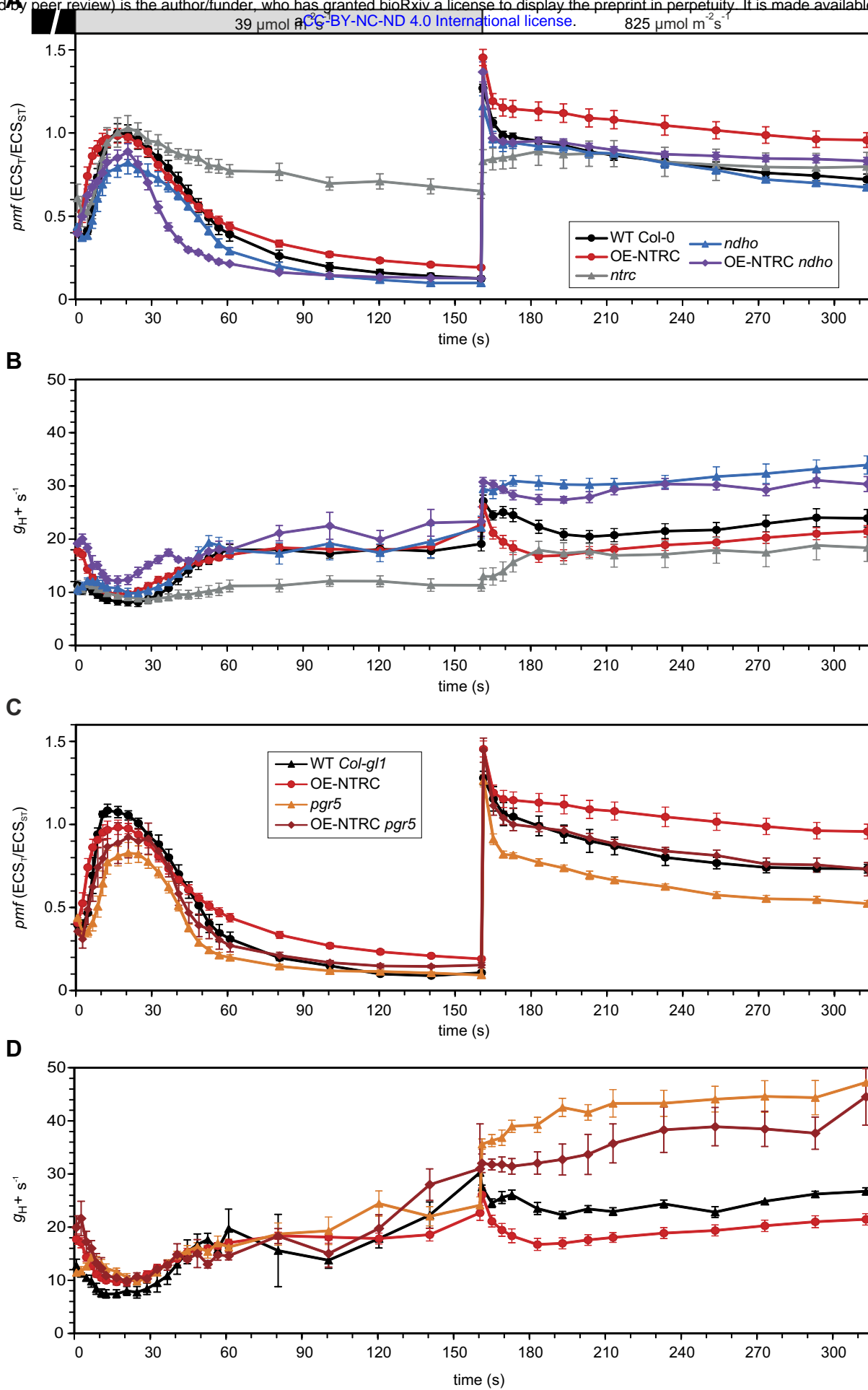


**Figure 7.** Formation and regulation the proton motive force during changes in light conditions.

**(A–B)** The *pmf* (A) and proton conductivity of the thylakoid membrane( $g_{H^+}$ ) (B) at specific time points during transitions from darkness to low actinic light ( $39 \mu\text{mol photons m}^{-2} \text{s}^{-1}$ ) and from low to high light ( $825 \mu\text{mol photons m}^{-2} \text{s}^{-1}$ ) in dark-adapted leaves of WT Col-0, OE-NTRC, *ntrc*, *ndho* and OE-NTRC *ndho*. The *pmf* and  $g_{H^+}$  were measured and calculated as explained in the legend for Figure 5. The graphs shown are averages from 4–13 individual measurements  $\pm$ SE.

**(C–D)** The *pmf* and  $g_{H^+}$  in dark-adapted leaves of WT Col-*gl1*, OE-NTRC, *pgr5* and OE-NTRC *pgr5*. The graphs shown are averages from 3–13 individual measurements  $\pm$ SE.

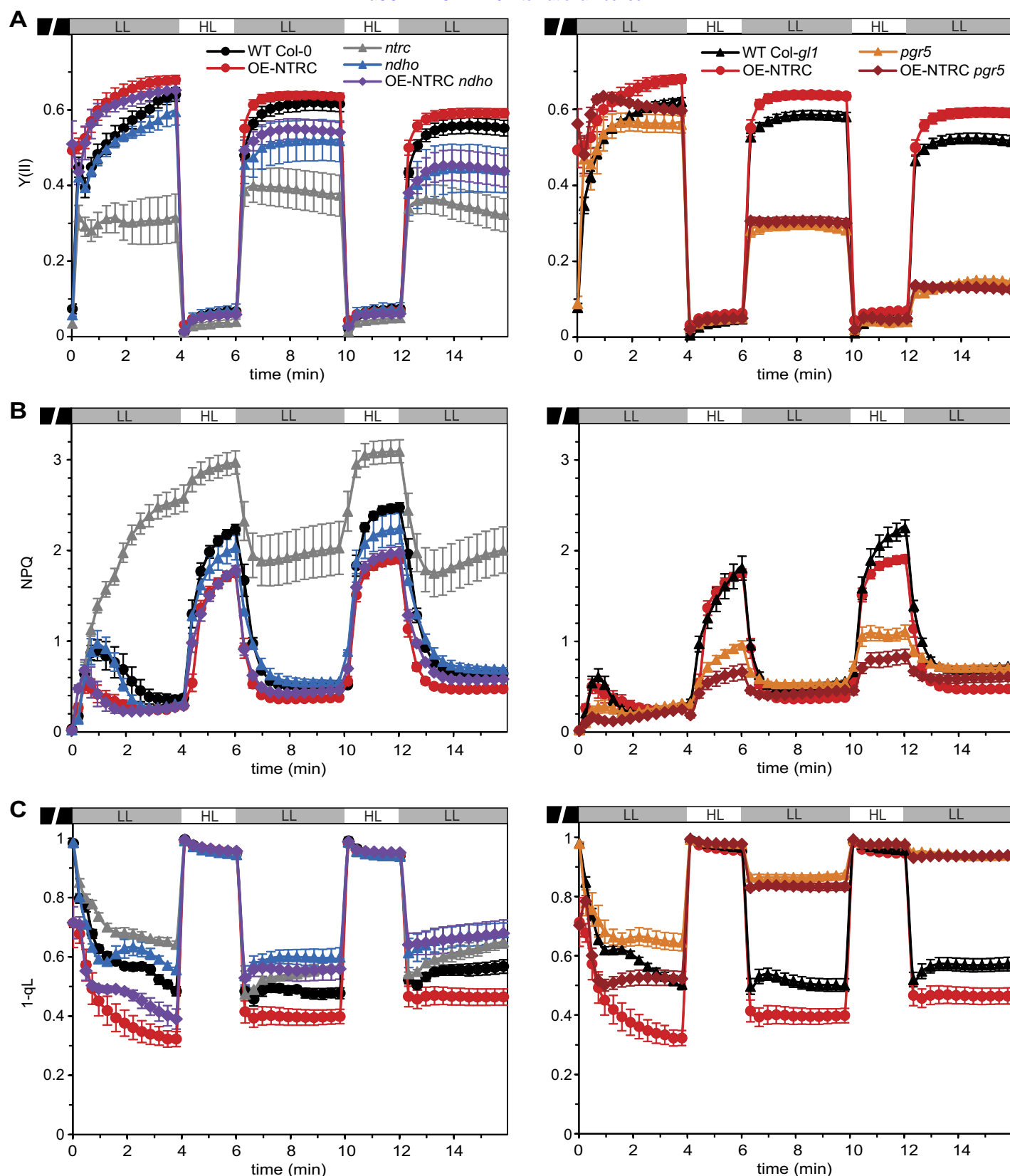


**Figure 8.** Analysis of Chlorophyll a fluorescence in fluctuating light.

**(A-C)** PSII yield (Y(II)) (A), non-photochemical quenching (NPQ) (B) and redox state of the PQ pool (1-qL) (C) in light conditions fluctuating between periods of low actinic light (LL, 39  $\mu\text{mol photons m}^{-2} \text{s}^{-1}$ ) and high light (HL, 825  $\mu\text{mol photons m}^{-2} \text{s}^{-1}$ ) in WT Col-0, OE-NTRC, *ntrc*, *ndho*, OE-NTRC *ndho*, WT Col-*gl1*, *pgr5* and OE-NTRC *pgr5*. Five weeks old plants were dark-adapted for 30 min before measuring fluorescence from detached leaves. All values are averages of 3–10 individual measurements  $\pm$  SE.

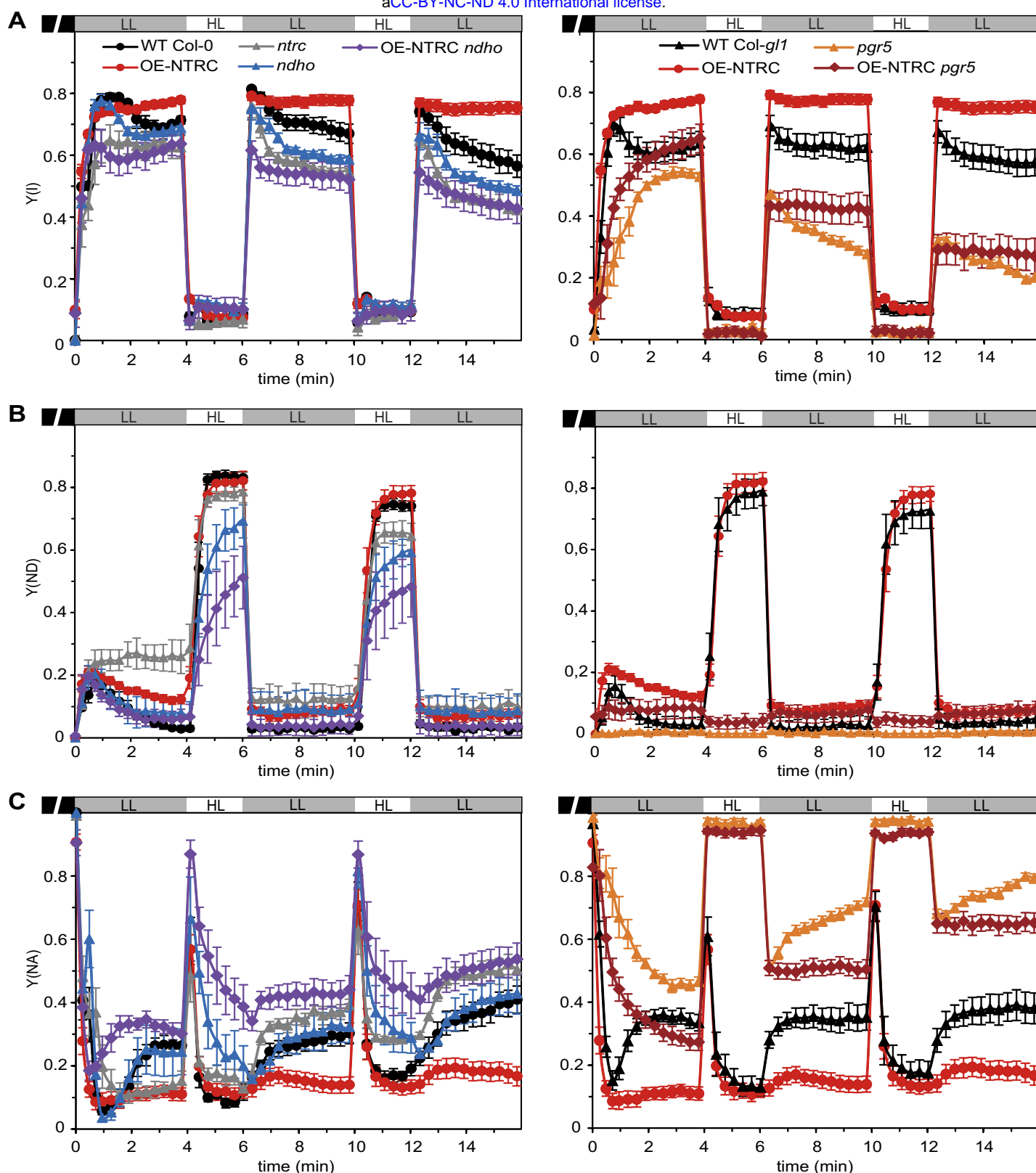


**Figure 9.** Analysis of P700 oxidation in fluctuating light.

**(A-C)** PSI yield (Y(I) (A), P700 oxidation (Y(ND)) (B) and PSI acceptor side limitation (Y(NA)) (C) in light conditions fluctuating between periods of low actinic light (LL, 39  $\mu\text{mol photons m}^{-2} \text{s}^{-1}$ ) and high light (HL, 825  $\mu\text{mol photons m}^{-2} \text{s}^{-1}$ ) in WT Col-0, OE-NTRC, *ntrc*, *ndho*, OE-NTRC *ndho*, WT Col-*gl1*, *pgr5* and OE-NTRC *pgr5*. Five weeks old plants were dark-adapted for 30 min before measuring fluorescence from detached leaves. All values are averages of 3–10 individual measurements  $\pm$ SE.

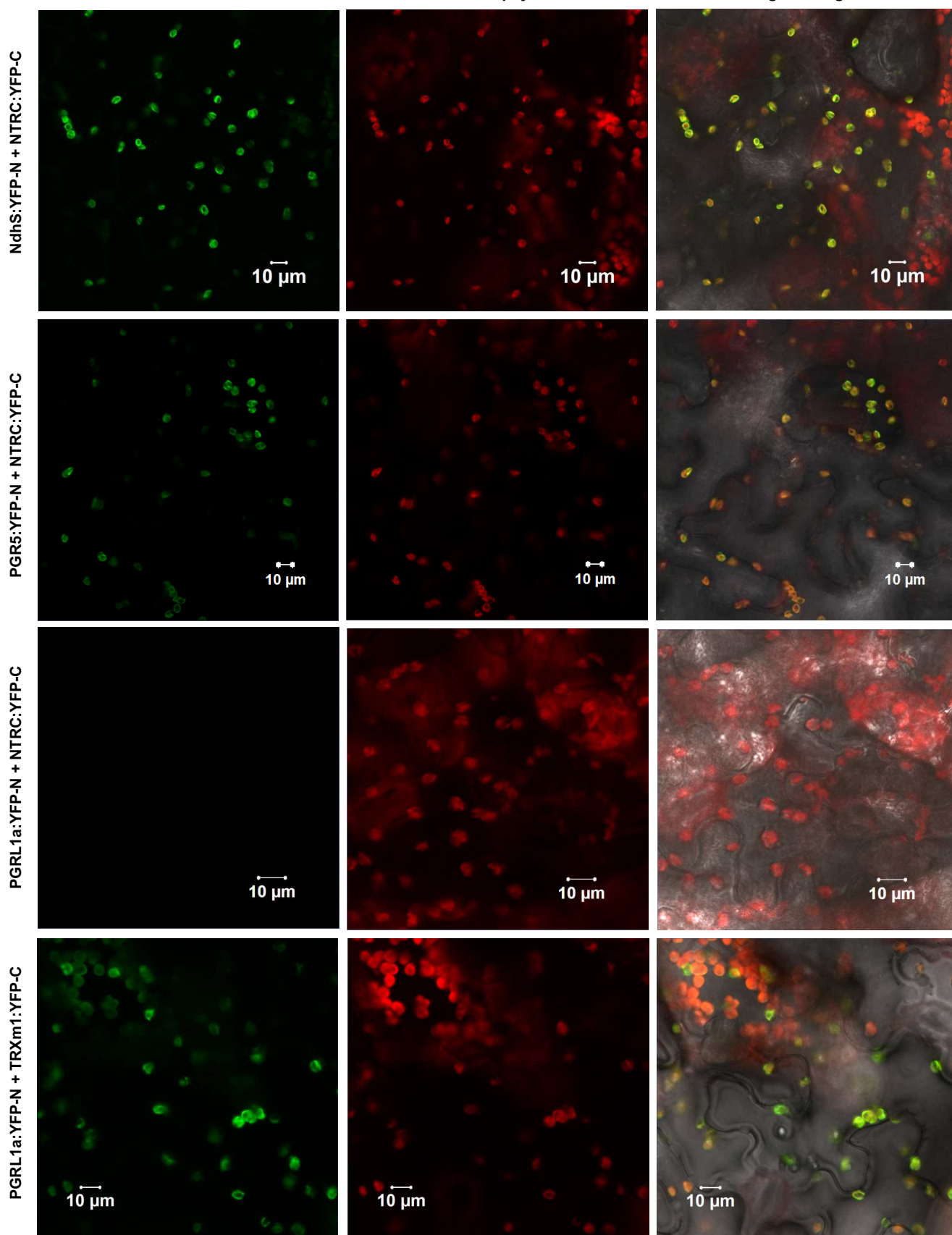


**Figure 10.** Bimolecular fluorescence complementation (BiFC) tests of *in planta* interactions between chloroplast TRXs and potential CEF target proteins.

The left panel shows yellow fluorescent protein (YFP) fluorescence in green, the middle panel Chlorophyll a autofluorescence in red and the right panel a merged image of YFP, chlorophyll and brightfield images. YFP-N and YFP-C indicate expression of a fusion proteins including the N-terminal and C-terminal parts of YFP, respectively, in tobacco (*Nicotiana benthamiana*) leaves.

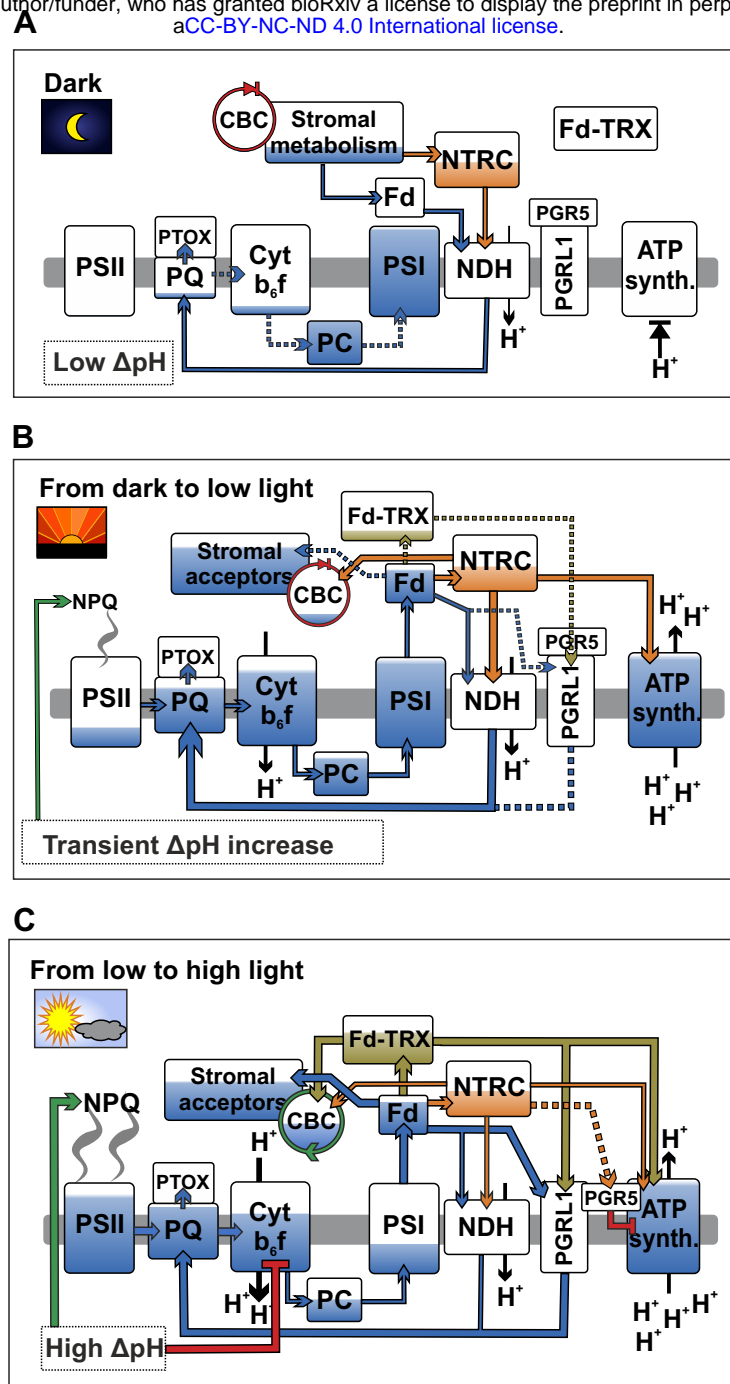


**Figure 11.** A schematic model of the role of chloroplast TRX systems in regulating CEF and the *pmf* during dark-to-light transitions and fluctuations in light conditions.

**(A–C)** Dark-adapted leaves (A), transition from dark to low light (B) and transition from low to high light (C). Blue color indicates the level of reduction, green and red arrows represent the activating and inhibitory effects, respectively, while orange represents the thiol regulation by NTRC and dark yellow by the Fd-TRX system. Thicker lines depict stronger effect than thin and dotted lines. For details see the text.

## Parsed Citations

**Allorent, G., Osorio, S., Vu, J.L., Falconet, D., Jouhet, J., Kuntz, M., Fernie, A.R., Lerbs-Mache, S., Macherel, D., Courtois, F., and Finazzi, G. (2015). Adjustments of embryonic photosynthetic activity modulate seed fitness in *Arabidopsis thaliana*. *New Phytol.* 205, 707-719.**

Pubmed: [Author and Title](#)

CrossRef: [Author and Title](#)

Google Scholar: [Author Only Title Only Author and Title](#)

**Armbruster, U., Correa Galvis, V., Kunz, H.H., and Strand, D.D. (2017). The regulation of the chloroplast proton motive force plays a key role for photosynthesis in fluctuating light. *Curr. Opin. Plant Biol.* 37, 56-62.**

Pubmed: [Author and Title](#)

CrossRef: [Author and Title](#)

Google Scholar: [Author Only Title Only Author and Title](#)

**Armbruster, U., Carrillo, L.R., Venema, K., Pavlovic, L., Schmidtman, E., Kornfeld, A., Jahns, P., Berry, J.A., Kramer, D.M., and Jonikas, M.C. (2014). Ion antiport accelerates photosynthetic acclimation in fluctuating light environments. *Nature Comm.* 5, 5439.**

Pubmed: [Author and Title](#)

CrossRef: [Author and Title](#)

Google Scholar: [Author Only Title Only Author and Title](#)

**Avenson, T., Cruz, J., Kanazawa, A., and Kramer, D. (2005). Regulating the proton budget of higher plant photosynthesis. *Proc. Natl. Acad. Sci. U. S. A.* 102, 9709-9713.**

Pubmed: [Author and Title](#)

CrossRef: [Author and Title](#)

Google Scholar: [Author Only Title Only Author and Title](#)

**Bailey, S., Walters, R.G., Jansson, S., and Horton, P. (2001). Acclimation of *Arabidopsis thaliana* to the light environment: the existence of separate low light and high light responses. *Planta* 213, 794-801.**

Pubmed: [Author and Title](#)

CrossRef: [Author and Title](#)

Google Scholar: [Author Only Title Only Author and Title](#)

**Balsera, M., Uberegui, E., Schürmann, P., and Buchanan, B.B. (2014). Evolutionary Development of Redox Regulation in Chloroplasts. *Antioxid. Redox Signal.* 21, 1327-1355.**

Pubmed: [Author and Title](#)

CrossRef: [Author and Title](#)

Google Scholar: [Author Only Title Only Author and Title](#)

**Bellafiore, S., Barneche, F., Peltier, G., and Rochaix, J. (2005). State transitions and light adaptation require chloroplast thylakoid protein kinase STN7. *Nature* 433, 892-895.**

Pubmed: [Author and Title](#)

CrossRef: [Author and Title](#)

Google Scholar: [Author Only Title Only Author and Title](#)

**Breyton, C., Nandha, B., Johnson, G.N., Joliot, P., and Finazzi, G. (2006). Redox modulation of cyclic electron flow around photosystem I in C3 plants. *Biochemistry (N. Y.)* 45, 13465-13475.**

Pubmed: [Author and Title](#)

CrossRef: [Author and Title](#)

Google Scholar: [Author Only Title Only Author and Title](#)

**Brooks, M.D., Sylak-Glassman, E.J., Fleming, G.R., and Niyogi, K.K. (2013). A thioredoxin-like/beta-propeller protein maintains the efficiency of light harvesting in *Arabidopsis*. *Proc. Natl. Acad. Sci. U. S. A.* 110, E2733-40.**

Pubmed: [Author and Title](#)

CrossRef: [Author and Title](#)

Google Scholar: [Author Only Title Only Author and Title](#)

**Buchanan, B.B. (2016). The Path to Thioredoxin and Redox Regulation in Chloroplasts. 67, 1-24.**

Pubmed: [Author and Title](#)

CrossRef: [Author and Title](#)

Google Scholar: [Author Only Title Only Author and Title](#)

**Carrillo, L.R., Froehlich, J.E., Cruz, J.A., Savage, L.J., and Kramer, D.M. (2016). Multi-level regulation of the chloroplast ATP synthase: the chloroplast NADPH thioredoxin reductase C (NTRC) is required for redox modulation specifically under low irradiance. *Plant J.* 87, 654-663.**

Pubmed: [Author and Title](#)

CrossRef: [Author and Title](#)

Google Scholar: [Author Only Title Only Author and Title](#)

**Collin, V., Issakidis-Bourguet, E., Marchand, C., Hirasawa, M., Lancelin, J., Knaff, D., and Miginiac-Maslow, M. (2003). The *Arabidopsis* plastidial thioredoxins - New functions and new insights into specificity. *J. Biol. Chem.* 278, 23747-23752.**

Pubmed: [Author and Title](#)

CrossRef: [Author and Title](#)

Google Scholar: [Author Only Title Only Author and Title](#)

**Courteille, A, Vesa, S., Sanz-Barrio, R., Cazale, A., Becuwe-Linka, N., Farran, I., Havaux, M., Rey, P., and Rumeau, D. (2013). Thioredoxin m4 Controls Photosynthetic Alternative Electron Pathways in Arabidopsis. Plant Physiol. 161, 508-520.**

Pubmed: [Author and Title](#)  
CrossRef: [Author and Title](#)  
Google Scholar: [Author Only Title Only Author and Title](#)

**Couturier, J., Chibani, K., Jacquot, J., and Rouhier, N. (2013). Cysteine-based redox regulation and signaling in plants. Front. Plant Sci. 4, 105.**

Pubmed: [Author and Title](#)  
CrossRef: [Author and Title](#)  
Google Scholar: [Author Only Title Only Author and Title](#)

**Cruz, J., Sacksteder, C., Kanazawa, A., and Kramer, D. (2001). Contribution of electric field (Delta psi) to steady-state transthylakoid proton motive force (pmf) in vitro and in vivo. Control of pmf parsing into Delta psi and Delta pH by ionic strength. Biochemistry (N. Y.) 40, 1226-1237.**

Pubmed: [Author and Title](#)  
CrossRef: [Author and Title](#)  
Google Scholar: [Author Only Title Only Author and Title](#)

**Cruz, J., Avenon, T., Kanazawa, A., Takizawa, K., Edwards, G., and Kramer, D. (2005). Plasticity in light reactions of photosynthesis for energy production and photoprotection. J. Exp. Bot. 56, 395-406.**

Pubmed: [Author and Title](#)  
CrossRef: [Author and Title](#)  
Google Scholar: [Author Only Title Only Author and Title](#)

**Da, Q., Sun, T., Wang, M., Jin, H., Li, M., Feng, D., Wang, J., Wang, H., and Liu, B. (2017). M-type thioredoxins are involved in the xanthophyll cycle and proton motive force to alter NPQ under low-light conditions in Arabidopsis. Plant Cell Rep.**

Pubmed: [Author and Title](#)  
CrossRef: [Author and Title](#)  
Google Scholar: [Author Only Title Only Author and Title](#)

**DalCorso, G., Pesaresi, P., Masiero, S., Aseeva, E., Schuenemann, D., Finazzi, G., Joliot, P., Barbato, R., and Leister, D. (2008). A complex containing PGRL1 and PGR5 is involved in the switch between linear and cyclic electron flow in Arabidopsis. Cell 132, 273-285.**

Pubmed: [Author and Title](#)  
CrossRef: [Author and Title](#)  
Google Scholar: [Author Only Title Only Author and Title](#)

**Davis, G.A., Kanazawa, A., Schoettler, M.A., Kohzuma, K., Froehlich, J.E., Rutherford, A.W., Satoh-Cruz, M., Minhas, D., Tietz, S., Dhingra, A., and Kramer, D.M. (2016). Limitations to photosynthesis by proton motive force-induced photosystem II photodamage. eLife 5, e16921.**

Pubmed: [Author and Title](#)  
CrossRef: [Author and Title](#)  
Google Scholar: [Author Only Title Only Author and Title](#)

**Demmig-Adams, B., Cohu, C.M., Muller, O., and Adams, W.W., 3rd (2012). Modulation of photosynthetic energy conversion efficiency in nature: from seconds to seasons. Photosynth Res. 113, 75-88.**

Pubmed: [Author and Title](#)  
CrossRef: [Author and Title](#)  
Google Scholar: [Author Only Title Only Author and Title](#)

**Fan, D., Nie, Q., Hope, A.B., Hillier, W., Pogson, B.J., and Chow, W.S. (2007). Quantification of cyclic electron flow around Photosystem I in spinach leaves during photosynthetic induction. Photosynthesis Res. 94, 347-357.**

Pubmed: [Author and Title](#)  
CrossRef: [Author and Title](#)  
Google Scholar: [Author Only Title Only Author and Title](#)

**Geigenberger, P., Thormählen, I., Daloso, D.M., and Fernie, A.R. (2017). The Unprecedented Versatility of the Plant Thioredoxin System. Trends Plant Sci. 22, 249-262.**

Pubmed: [Author and Title](#)  
CrossRef: [Author and Title](#)  
Google Scholar: [Author Only Title Only Author and Title](#)

**Gollan, P.J., Lima-Melo, Y., Tiwari, A., Tikkanen, M., and Aro, E. (2017). Interaction between photosynthetic electron transport and chloroplast sinks triggers protection and signalling important for plant productivity. Philos Trans R Soc Lond B Biol Sci 372, , doi/10.1098/rstb.2016.0390.**

Pubmed: [Author and Title](#)  
CrossRef: [Author and Title](#)  
Google Scholar: [Author Only Title Only Author and Title](#)

**Gotoh, E., Matsumoto, M., Ogawa, K., Kobayashi, Y., and Tsuyama, M. (2010). A qualitative analysis of the regulation of cyclic electron flow around photosystem I from the post-illumination chlorophyll fluorescence transient in Arabidopsis: a new platform for the in vivo investigation of the chloroplast redox state. Photosynthesis Res. 103, 111-123.**

Pubmed: [Author and Title](#)  
CrossRef: [Author and Title](#)

Google Scholar: [Author Only](#) [Title Only](#) [Author and Title](#)

**Grieco, M., Tikkanen, M., Paakkanen, V., Kangasjarvi, S., and Aro, E.M. (2012). Steady-state phosphorylation of light-harvesting complex II proteins preserves photosystem I under fluctuating white light. *Plant Physiol.* 160, 1896-1910.**

Pubmed: [Author and Title](#)

CrossRef: [Author and Title](#)

Google Scholar: [Author Only](#) [Title Only](#) [Author and Title](#)

**Hall, M., Mata-Cabana, A., Akerlund, H.E., Florencio, F.J., Schroder, W.P., Lindahl, M., and Kieselbach, T. (2010). Thioredoxin targets of the plant chloroplast lumen and their implications for plastid function. *Proteomics* 10, 987-1001.**

Pubmed: [Author and Title](#)

CrossRef: [Author and Title](#)

Google Scholar: [Author Only](#) [Title Only](#) [Author and Title](#)

**Hallin, E.I., Guo, K., and Åkerlund, H. (2015). Violaxanthin de-epoxidase disulphides and their role in activity and thermal stability. *Photosynthesis Res.* 124, 191-198.**

Pubmed: [Author and Title](#)

CrossRef: [Author and Title](#)

Google Scholar: [Author Only](#) [Title Only](#) [Author and Title](#)

**Hertle, A.P., Blunder, T., Wunder, T., Pesaresi, P., Pribil, M., Armbruster, U., and Leister, D. (2013). PGRL1 Is the Elusive Ferredoxin-Plastoquinone Reductase in Photosynthetic Cyclic Electron Flow. *Mol. Cell* 49, 511-523.**

Pubmed: [Author and Title](#)

CrossRef: [Author and Title](#)

Google Scholar: [Author Only](#) [Title Only](#) [Author and Title](#)

**Hirasawa, M., Schurmann, P., Jacquot, J., Manieri, W., Jacquot, P., Keryer, E., Hartman, F., and Knaff, D. (1999). Oxidation-reduction properties of chloroplast thioredoxins, Ferredoxin : Thioredoxin reductase, and thioredoxin f-regulated enzymes. *Biochemistry (N. Y.)* 38, 5200-5205.**

Pubmed: [Author and Title](#)

CrossRef: [Author and Title](#)

Google Scholar: [Author Only](#) [Title Only](#) [Author and Title](#)

**Horvath, E., Peter, S., Joet, T., Rumeau, D., Cournac, L., Horvath, G., Kavanagh, T., Schafer, C., Peltier, G., and Medgyesy, P. (2000). Targeted inactivation of the plastid ndhB gene in tobacco results in an enhanced sensitivity of photosynthesis to moderate stomatal closure. *Plant Physiol.* 123, 1337-1349.**

Pubmed: [Author and Title](#)

CrossRef: [Author and Title](#)

Google Scholar: [Author Only](#) [Title Only](#) [Author and Title](#)

**Johnson, G.N. (2011). Physiology of PSI cyclic electron transport in higher plants. 1807, 384-389, doi/https://doi.org/10.1016/j.bbabi.2010.11.009.**

Pubmed: [Author and Title](#)

CrossRef: [Author and Title](#)

Google Scholar: [Author Only](#) [Title Only](#) [Author and Title](#)

**Joliot, P. and Joliot, A (2002). Cyclic electron transfer in plant leaf. *Proc. Natl. Acad. Sci. U. S. A* 99, 10209-10214.**

Pubmed: [Author and Title](#)

CrossRef: [Author and Title](#)

Google Scholar: [Author Only](#) [Title Only](#) [Author and Title](#)

**Joliot, P. and Johnson, G.N. (2011). Regulation of cyclic and linear electron flow in higher plants. *Proc. Natl. Acad. Sci. U. S. A* 108, 13317-13322.**

Pubmed: [Author and Title](#)

CrossRef: [Author and Title](#)

Google Scholar: [Author Only](#) [Title Only](#) [Author and Title](#)

**Junesch, U. and Gräber, P. (1991). The Rate of ATP-Synthesis as a Function of Delta-pH and Delta-Psi Catalyzed by the Active, Reduced H<sup>+</sup>-Atpase from Chloroplasts. *FEBS Lett.* 294, 275-278.**

Pubmed: [Author and Title](#)

CrossRef: [Author and Title](#)

Google Scholar: [Author Only](#) [Title Only](#) [Author and Title](#)

**Kanazawa, A., Ostendorf, E., Kohzuma, K., Hoh, D., Strand, D.D., Sato-Cruz, M., Savage, L., Cruz, J.A, Fisher, N., Froehlich, J.E., and Kramer, D.M. (2017). Chloroplast ATP Synthase Modulation of the Thylakoid Proton Motive Force: Implications for Photosystem I and Photosystem II Photoprotection. *Front. Plant Sci.* 8, 719.**

Pubmed: [Author and Title](#)

CrossRef: [Author and Title](#)

Google Scholar: [Author Only](#) [Title Only](#) [Author and Title](#)

**Kirchsteiger, K., Pulido, P., Gonzalez, M., and Javier Cejudo, F. (2009). NADPH Thioredoxin Reductase C Controls the Redox Status of Chloroplast 2-Cys Peroxiredoxins in Arabidopsis thaliana. *Mol. Plant.* 2, 298-307.**

Pubmed: [Author and Title](#)

CrossRef: [Author and Title](#)

Google Scholar: [Author Only](#) [Title Only](#) [Author and Title](#)

**Klughammer, C., Siebke, K., and Schreiber, U. (2013). Continuous ECS-indicated recording of the proton-motive charge flux in leaves. Photosynthesis Res. 117, 471-487.**

Pubmed: [Author and Title](#)

CrossRef: [Author and Title](#)

Google Scholar: [Author Only Title Only Author and Title](#)

**Kono, M. and Terashima, I. (2014). Long-term and short-term responses of the photosynthetic electron transport to fluctuating light. J. Photochem. Photobiol. B. 137, 89-99.**

Pubmed: [Author and Title](#)

CrossRef: [Author and Title](#)

Google Scholar: [Author Only Title Only Author and Title](#)

**Kou, J., Takahashi, S., Fan, D., Badger, M.R., and Chow, W.S. (2015). Partially dissecting the steady-state electron fluxes in Photosystem I in wild-type and pgr5 and ndh mutants of Arabidopsis. Front. Plant Sci. 6, 758.**

Pubmed: [Author and Title](#)

CrossRef: [Author and Title](#)

Google Scholar: [Author Only Title Only Author and Title](#)

**Kramer, D.M. and Crofts, A.R. (1989). Activation of the Chloroplast Atpase Measured by the Electrochromic Change in Leaves of Intact Plants. Biochim. Biophys. Acta 976, 28-41.**

Pubmed: [Author and Title](#)

CrossRef: [Author and Title](#)

Google Scholar: [Author Only Title Only Author and Title](#)

**Kramer, D.M., Johnson, G., Kiirats, O., and Edwards, G.E. (2004). New fluorescence parameters for the determination of Q(A) redox state and excitation energy fluxes. Photosynthesis Res. 79, 209-218.**

Pubmed: [Author and Title](#)

CrossRef: [Author and Title](#)

Google Scholar: [Author Only Title Only Author and Title](#)

**Kramer, D., Wise, R., Frederick, J., Alm, D., Hesketh, J., Ort, D., and Crofts, A. (1990). Regulation of Coupling Factor in Field-Grown Sunflower - a Redox Model Relating Coupling Factor Activity to the Activities of Other Thioredoxin-Dependent Chloroplast Enzymes. Photosynthesis Res. 26, 213-222.**

Pubmed: [Author and Title](#)

CrossRef: [Author and Title](#)

Google Scholar: [Author Only Title Only Author and Title](#)

**Leister, D. and Shikanai, T. (2013). Complexities and protein complexes in the antimycin A-sensitive pathway of cyclic electron flow in plants. Front. Plant Sci. 4, 161.**

Pubmed: [Author and Title](#)

CrossRef: [Author and Title](#)

Google Scholar: [Author Only Title Only Author and Title](#)

**Lepistö, A., Kangasjärvi, S., Luomala, E., Brader, G., Sipari, N., Keränen, M., Keinänen, M., and Rintamäki, E. (2009). Chloroplast NADPH-Thioredoxin Reductase Interacts with Photoperiodic Development in Arabidopsis. Plant Physiol. 149, 1261-1276.**

Pubmed: [Author and Title](#)

CrossRef: [Author and Title](#)

Google Scholar: [Author Only Title Only Author and Title](#)

**Lepistö, A., Pakula, E., Toivola, J., Krieger-Liszkay, A., Vignols, F., and Rintamäki, E. (2013). Deletion of chloroplast NADPH-dependent thioredoxin reductase results in inability to regulate starch synthesis and causes stunted growth under short-day photoperiods. J. Exp. Bot. 64, 3843-3854.**

Pubmed: [Author and Title](#)

CrossRef: [Author and Title](#)

Google Scholar: [Author Only Title Only Author and Title](#)

**Livingston, A.K., Cruz, J.A., Kohzuma, K., Dhingra, A., and Kramer, D.M. (2010). An Arabidopsis Mutant with High Cyclic Electron Flow around Photosystem I (hcef) Involving the NADPH Dehydrogenase Complex. Plant Cell 22, 221-233.**

Pubmed: [Author and Title](#)

CrossRef: [Author and Title](#)

Google Scholar: [Author Only Title Only Author and Title](#)

**Martin, M., Noarbe, D.M., Serrot, P.H., and Sabater, B. (2015). The rise of the photosynthetic rate when light intensity increases is delayed in ndh gene-defective tobacco at high but not at low CO<sub>2</sub> concentrations. Front. Plant Sci. 6, 34.**

Pubmed: [Author and Title](#)

CrossRef: [Author and Title](#)

Google Scholar: [Author Only Title Only Author and Title](#)

**Martinsuo, P., Pursiheimo, S., Aro, E., and Rintamäki, E. (2003). Dithiol oxidant and disulfide reductant dynamically regulate the phosphorylation of light-harvesting complex II proteins in thylakoid membranes. Plant Physiol. 133, 37-46.**

Pubmed: [Author and Title](#)

CrossRef: [Author and Title](#)

Google Scholar: [Author Only Title Only Author and Title](#)

**McKinney, D., Buchanan, B., and Wolosiuk, R. (1978). Activation of Chloroplast Atpase by Reduced Thioredoxin. Phytochemistry 17,**

794-795.

Pubmed: [Author and Title](#)  
CrossRef: [Author and Title](#)  
Google Scholar: [Author Only](#) [Title Only](#) [Author and Title](#)

**Miyake, C., Shinzaki, Y., Miyata, M., and Tomizawa, K. (2004). Enhancement of cyclic electron flow around PSI at high light and its contribution to the induction of non-photochemical quenching of chl fluorescence in intact leaves of tobacco plants. *Plant Cell Physiol* 45, 1426-1433.**

Pubmed: [Author and Title](#)  
CrossRef: [Author and Title](#)  
Google Scholar: [Author Only](#) [Title Only](#) [Author and Title](#)

**Munekage, Y., Hojo, M., Meurer, J., Endo, T., Tasaka, M., and Shikanai, T. (2002). PGR5 is involved in cyclic electron flow around photosystem I and is essential for photoprotection in Arabidopsis. *Cell* 110, 361-371.**

Pubmed: [Author and Title](#)  
CrossRef: [Author and Title](#)  
Google Scholar: [Author Only](#) [Title Only](#) [Author and Title](#)

**Munekage, Y., Hashimoto, M., Miyake, C., Tomizawa, K., Endo, T., Tasaka, M., and Shikanai, T. (2004). Cyclic electron flow around photosystem I is essential for photosynthesis. *Nature* 429, 579-582.**

Pubmed: [Author and Title](#)  
CrossRef: [Author and Title](#)  
Google Scholar: [Author Only](#) [Title Only](#) [Author and Title](#)

**Murashige, T. and Skoog, F. (1962). A Revised Medium for Rapid Growth and Bio Assays with Tobacco Tissue Cultures. *Physiol. Plantarum* 15, 473-497.**

Pubmed: [Author and Title](#)  
CrossRef: [Author and Title](#)  
Google Scholar: [Author Only](#) [Title Only](#) [Author and Title](#)

**Nalin, C. and McCarty, R. (1984). Role of a Disulfide Bond in the Gamma-Subunit in Activation of the Atpase of Chloroplast Coupling Factor-i. *J. Biol. Chem* 259, 7275-7280.**

Pubmed: [Author and Title](#)  
CrossRef: [Author and Title](#)  
Google Scholar: [Author Only](#) [Title Only](#) [Author and Title](#)

**Naranjo, B., Mignee, C., Krieger-Liszky, A., Hornero-Mendez, D., Gallardo-Guerrero, L., Javier Cejudo, F., and Lindahl, M. (2016). The chloroplast NADPH thioredoxin reductase C, NTRC, controls non-photochemical quenching of light energy and photosynthetic electron transport in Arabidopsis. *Plant Cell Environ.* 39, 804-822.**

Pubmed: [Author and Title](#)  
CrossRef: [Author and Title](#)  
Google Scholar: [Author Only](#) [Title Only](#) [Author and Title](#)

**Nikkanen, L. and Rintamäki, E. (2014). Thioredoxin-dependent regulatory networks in chloroplasts under fluctuating light conditions. *Philos. Trans. R. Soc. B-Biol. Sci.* 369, 20130224.**

Pubmed: [Author and Title](#)  
CrossRef: [Author and Title](#)  
Google Scholar: [Author Only](#) [Title Only](#) [Author and Title](#)

**Nikkanen, L., Toivola, J., and Rintamäki, E. (2016). Crosstalk between chloroplast thioredoxin systems in regulation of photosynthesis. *Plant Cell Environ.* 39, 1691-1705.**

Pubmed: [Author and Title](#)  
CrossRef: [Author and Title](#)  
Google Scholar: [Author Only](#) [Title Only](#) [Author and Title](#)

**Niyogi, K.K. and Truong, T.B. (2013). Evolution of flexible non-photochemical quenching mechanisms that regulate light harvesting in oxygenic photosynthesis. *Curr. Opin. Plant Biol.* 16, 307-314, doi/<https://doi.org/10.1016/j.pbi.2013.03.011>.**

Pubmed: [Author and Title](#)  
CrossRef: [Author and Title](#)  
Google Scholar: [Author Only](#) [Title Only](#) [Author and Title](#)

**Okegawa, Y., Kagawa, Y., Kobayashi, Y., and Shikanai, T. (2008). Characterization of factors affecting the activity of photosystem I cyclic electron transport in chloroplasts. *Plant Cell Physiol* 49, 825-834.**

Pubmed: [Author and Title](#)  
CrossRef: [Author and Title](#)  
Google Scholar: [Author Only](#) [Title Only](#) [Author and Title](#)

**Peltier, G., Aro, E., and Shikanai, T. (2016). NDH-1 and NDH-2 Plastoquinone Reductases in Oxygenic Photosynthesis. *Annual Review of Plant Biology, Annu. Rev. Plant Biol.* 67, 55-80.**

Pubmed: [Author and Title](#)  
CrossRef: [Author and Title](#)  
Google Scholar: [Author Only](#) [Title Only](#) [Author and Title](#)

**Perez-Ruiz, J.M., Spinola, M.C., Kirchsteiger, K., Moreno, J., Sahrawy, M., and Cejudo, F.J. (2006). Rice NTRC is a high-efficiency redox system for chloroplast protection against oxidative damage. *Plant Cell* 18, 2356-2368.**

Pubmed: [Author and Title](#)  
 CrossRef: [Author and Title](#)  
 Google Scholar: [Author Only Title Only Author and Title](#)

**Pérez-Ruiz, J.M., Naranjo, B., Ojeda, V., Guinea, M., and Cejudo, F.J. (2017). NTRC-dependent redox balance of 2-Cys peroxiredoxins is needed for optimal function of the photosynthetic apparatus. Proc. Natl. Acad. Sci. U. S. A 114, 12069-12074.**

Pubmed: [Author and Title](#)  
 CrossRef: [Author and Title](#)  
 Google Scholar: [Author Only Title Only Author and Title](#)

**Petroutsos, D., Terauchi, A.M., Busch, A., Hirschmann, I., Merchant, S.S., Finazzi, G., and Hippler, M. (2009). PGRL1 Participates in Iron-induced Remodeling of the Photosynthetic Apparatus and in Energy Metabolism in Chlamydomonas reinhardtii. J. Biol. Chem. 284, 32770-32781.**

Pubmed: [Author and Title](#)  
 CrossRef: [Author and Title](#)  
 Google Scholar: [Author Only Title Only Author and Title](#)

**Porra, R., Thompson, W., and Kriedemann, P. (1989). Determination of Accurate Extinction Coefficients and Simultaneous-Equations for Assaying Chlorophyll-a and Chlorophyll-B Extracted with 4 Different Solvents - Verification of the Concentration of Chlorophyll Standards by Atomic-Absorption Spectroscopy. Biochim. Biophys. Acta 975, 384-394.**

Pubmed: [Author and Title](#)  
 CrossRef: [Author and Title](#)  
 Google Scholar: [Author Only Title Only Author and Title](#)

**Pulido, P., Spinola, M.C., Kirchsteiger, K., Guinea, M., Belen Pascual, M., Sahrawy, M., Sandalio, L.M., Dietz, K., Gonzalez, M., and Cejudo, F.J. (2010). Functional analysis of the pathways for 2-Cys peroxiredoxin reduction in Arabidopsis thaliana chloroplasts. J. Exp. Bot. 61, 4043-4054.**

Pubmed: [Author and Title](#)  
 CrossRef: [Author and Title](#)  
 Google Scholar: [Author Only Title Only Author and Title](#)

**Rintamäki, E., Salonen, M., Suoranta, U., Carlberg, I., Andersson, B., and Aro, E. (1997). Phosphorylation of light-harvesting complex II and photosystem II core proteins shows different irradiance-dependent regulation in vivo - Application of phosphothreonine antibodies to analysis of thylakoid phosphoproteins. J. Biol. Chem. 272, 30476-30482.**

Pubmed: [Author and Title](#)  
 CrossRef: [Author and Title](#)  
 Google Scholar: [Author Only Title Only Author and Title](#)

**Rintamäki, E., Martinsuo, P., Pursiheimo, S., and Aro, E. (2000). Cooperative regulation of light-harvesting complex II phosphorylation via the plastoquinol and ferredoxin-thioredoxin system in chloroplasts. Proc. Natl. Acad. Sci. U. S. A 97, 11644-11649.**

Pubmed: [Author and Title](#)  
 CrossRef: [Author and Title](#)  
 Google Scholar: [Author Only Title Only Author and Title](#)

**Rochaix, J. (2011). Regulation of photosynthetic electron transport. Biochim. Biophys. Acta-Bioenerg. 1807, 375-383.**

Pubmed: [Author and Title](#)  
 CrossRef: [Author and Title](#)  
 Google Scholar: [Author Only Title Only Author and Title](#)

**Ruban, A.V. (2016). Nonphotochemical Chlorophyll Fluorescence Quenching: Mechanism and Effectiveness in Protecting Plants from Photodamage. Plant Physiol. 170, 1903-1916.**

Pubmed: [Author and Title](#)  
 CrossRef: [Author and Title](#)  
 Google Scholar: [Author Only Title Only Author and Title](#)

**Ruban, A.V. and Johnson, M.P. (2009). Dynamics of higher plant photosystem cross-section associated with state transitions. Photosynthesis Res. 99, 173-183.**

Pubmed: [Author and Title](#)  
 CrossRef: [Author and Title](#)  
 Google Scholar: [Author Only Title Only Author and Title](#)

**Rumeau, D., Becuwe-Linka, N., Beyly, A., Louwagie, M., Garin, J., and Peltier, G. (2005). New subunits NDH-M, -N, and -O, encoded by nuclear genes, are essential for plastid Ndh complex functioning in higher plants. Plant Cell 17, 219-232.**

Pubmed: [Author and Title](#)  
 CrossRef: [Author and Title](#)  
 Google Scholar: [Author Only Title Only Author and Title](#)

**Schneider, C.A., Rasband, W.S., and Eliceiri, K.W. (2012). NIH Image to ImageJ: 25 years of image analysis. 9, 671-675.**

Pubmed: [Author and Title](#)  
 CrossRef: [Author and Title](#)  
 Google Scholar: [Author Only Title Only Author and Title](#)

**Schreiber, U. and Klughammer, C. (2008). New accessory for the DUAL-PAM-100: The P515/535 module and examples of its application. PAM Application Notes 1, 1-10.**

Pubmed: [Author and Title](#)

CrossRef: [Author and Title](#)

Google Scholar: [Author Only Title Only Author and Title](#)

**Schürmann, P. and Buchanan, B.B. (2008). The ferredoxin/thioredoxin system of oxygenic photosynthesis. *Antioxid. Redox Signal.* 10, 1235-1273.**

Pubmed: [Author and Title](#)

CrossRef: [Author and Title](#)

Google Scholar: [Author Only Title Only Author and Title](#)

**Serrato, A.J., Perez-Ruiz, J.M., Spinola, M.C., and Cejudo, F.J. (2004). A novel NADPH thioredoxin reductase, localized in the chloroplast, which deficiency causes hypersensitivity to abiotic stress in *Arabidopsis thaliana*. *J. Biol. Chem.* 279, 43821-43827.**

Pubmed: [Author and Title](#)

CrossRef: [Author and Title](#)

Google Scholar: [Author Only Title Only Author and Title](#)

**Shapiguzov, A., Chai, X., Fucile, G., Longoni, P., Zhang, L., and Rochaix, J.-. (2016). Activation of the Stt7/STN7 Kinase through Dynamic Interactions with the Cytochrome b(6)f Complex (vol 171, pg 82, 2016). *Plant Physiol.* 171, 1533-1533.**

Pubmed: [Author and Title](#)

CrossRef: [Author and Title](#)

Google Scholar: [Author Only Title Only Author and Title](#)

**Shikanai, T., Endo, T., Hashimoto, T., Yamada, Y., Asada, K., and Yokota, A. (1998). Directed disruption of the tobacco *ndhB* gene impairs cyclic electron flow around photosystem I. *Proc. Natl. Acad. Sci. U. S. A.* 95, 9705-9709.**

Pubmed: [Author and Title](#)

CrossRef: [Author and Title](#)

Google Scholar: [Author Only Title Only Author and Title](#)

**Shikanai, T. (2016). Chloroplast NDH: A different enzyme with a structure similar to that of respiratory NADH dehydrogenase. *Biochim. Biophys. Acta-Bioenerg.* 1857, 1015-1022.**

Pubmed: [Author and Title](#)

CrossRef: [Author and Title](#)

Google Scholar: [Author Only Title Only Author and Title](#)

**Shikanai, T. and Yamamoto, H. (2017). Contribution of Cyclic and Pseudo-cyclic Electron Transport to the Formation of Proton Motive Force in Chloroplasts. *Mol. Plant.* 10, 20-29.**

Pubmed: [Author and Title](#)

CrossRef: [Author and Title](#)

Google Scholar: [Author Only Title Only Author and Title](#)

**Sievers, F., Wilm, A., Dineen, D., Gibson, T.J., Karplus, K., Li, W., Lopez, R., McWilliam, H., Remmert, M., Soeding, J., Thompson, J.D., and Higgins, D.G. (2011). Fast, scalable generation of high-quality protein multiple sequence alignments using Clustal Omega. *7*, 539.**

Pubmed: [Author and Title](#)

CrossRef: [Author and Title](#)

Google Scholar: [Author Only Title Only Author and Title](#)

**Stirbet, A., Riznichenko, G.Y., Rubin, A.B., and Govindjee (2014). Modeling chlorophyll a fluorescence transient: relation to photosynthesis. *Biochemistry (Mosc)* 79, 291-323.**

Pubmed: [Author and Title](#)

CrossRef: [Author and Title](#)

Google Scholar: [Author Only Title Only Author and Title](#)

**Strand, D.D., Fisher, N., and Kramer, D.M. (2017a). The higher plant plastid NAD(P)H dehydrogenase-like complex (NDH) is a high efficiency proton pump that increases ATP production by cyclic electron flow. *J. Biol. Chem.* 292, 11850-11860.**

Pubmed: [Author and Title](#)

CrossRef: [Author and Title](#)

Google Scholar: [Author Only Title Only Author and Title](#)

**Strand, D.D., Livingston, A.K., Satoh-Cruz, M., Froehlich, J.E., Maurino, V.G., and Kramer, D.M. (2015). Activation of cyclic electron flow by hydrogen peroxide in vivo. *Proc. Natl. Acad. Sci. U. S. A.* 112, 5539-5544.**

Pubmed: [Author and Title](#)

CrossRef: [Author and Title](#)

Google Scholar: [Author Only Title Only Author and Title](#)

**Strand, D.D., Fisher, N., Davis, G.A., and Kramer, D.M. (2016a). Redox regulation of the antimycin A sensitive pathway of cyclic electron flow around photosystem I in higher plant thylakoids. *Biochim. Biophys. Acta-Bioenerg.* 1857, 1-6.**

Pubmed: [Author and Title](#)

CrossRef: [Author and Title](#)

Google Scholar: [Author Only Title Only Author and Title](#)

**Strand, D.D., Fisher, N., and Kramer, D.M. (2016b). Distinct Energetics and Regulatory Functions of the Two Major Cyclic Electron Flow Pathways in Chloroplasts In Chloroplasts: Current Research and Future Trends, Kirchhoff, H., ed (WYMONDHAM; 32 HEWTTTS LANE, WYMONDHAM NR 18 0JA, ENGLAND: CAISTER ACADEMIC PRESS) pp. 89-100.**

Pubmed: [Author and Title](#)

CrossRef: [Author and Title](#)

Google Scholar: [Author Only Title Only Author and Title](#)

**Strand, D.D., Livingston, A.K., Satoh-Cruz, M., Koepke, T., Enlow, H.M., Fisher, N., Froehlich, J.E., Cruz, J.A., Minhas, D., Hixson, K.K., Kohzuma, K., Lipton, M., Dhingra, A., and Kramer, D.M. (2017b). Defects in the Expression of Chloroplast Proteins Leads to H2O2 Accumulation and Activation of Cyclic Electron Flow around Photosystem I. *Front. Plant Sci.* 7, 2073.**

Pubmed: [Author and Title](#)  
CrossRef: [Author and Title](#)  
Google Scholar: [Author Only](#) [Title Only](#) [Author and Title](#)

**Suorsa, M., Jarvi, S., Grieco, M., Nurmi, M., Pietrzykowska, M., Rantala, M., Kangasjarvi, S., Paakkanen, V., Tikkanen, M., Jansson, S., and Aro, E. (2012). PROTON GRADIENT REGULATION5 Is Essential for Proper Acclimation of Arabidopsis Photosystem I to Naturally and Artificially Fluctuating Light Conditions. *Plant Cell* 24, 2934-2948.**

Pubmed: [Author and Title](#)  
CrossRef: [Author and Title](#)  
Google Scholar: [Author Only](#) [Title Only](#) [Author and Title](#)

**Suorsa, M., Grieco, M., Järvi, S., Gollan, P.J., Kangasjärvi, S., Tikkanen, M., and Aro, E. (2013). PGR5 ensures photosynthetic control to safeguard photosystem I under fluctuating light conditions. *Plant Signal Behav* 8, e22714.**

Pubmed: [Author and Title](#)  
CrossRef: [Author and Title](#)  
Google Scholar: [Author Only](#) [Title Only](#) [Author and Title](#)

**Suorsa, M. (2015). Cyclic electron flow provides acclimatory plasticity for the photosynthetic machinery under various environmental conditions and developmental stages. *Front. Plant Sci.* 6, 800.**

Pubmed: [Author and Title](#)  
CrossRef: [Author and Title](#)  
Google Scholar: [Author Only](#) [Title Only](#) [Author and Title](#)

**Suorsa, M., Rossi, F., Tadini, L., Labs, M., Colombo, M., Jahns, P., Kater, M.M., Leister, D., Finazzi, G., Aro, E., Barbato, R., and Pesaresi, P. (2016). PGR5-PGRL1-Dependent Cyclic Electron Transport Modulates Linear Electron Transport Rate in Arabidopsis thaliana. *Mol. Plant.* 9, 271-288.**

Pubmed: [Author and Title](#)  
CrossRef: [Author and Title](#)  
Google Scholar: [Author Only](#) [Title Only](#) [Author and Title](#)

**Thormählen, I., Meitzel, T., Groysman, J., Ochsner, A.B., von Roepenack-Lahaye, E., Naranjo, B., Cejudo, F.J., and Geigenberger, P. (2015). Thioredoxin f1 and NADPH-dependent thioredoxin reductase C have overlapping functions in regulating photosynthetic metabolism and plant growth in response to varying light conditions. *Plant Physiol.* 169, 1766-1786.**

Pubmed: [Author and Title](#)  
CrossRef: [Author and Title](#)  
Google Scholar: [Author Only](#) [Title Only](#) [Author and Title](#)

**Thormählen, I., Zupok, A., Rescher, J., Leger, J., Weissenberger, S., Groysman, J., Orwat, A., Chatel-Innocenti, G., Issakidis-Bourguet, E., Armbruster, U., and Geigenberger, P. (2017). Thioredoxins Play a Crucial Role in Dynamic Acclimation of Photosynthesis in Fluctuating Light. *Mol. Plant.* 10, 168-182.**

Pubmed: [Author and Title](#)  
CrossRef: [Author and Title](#)  
Google Scholar: [Author Only](#) [Title Only](#) [Author and Title](#)

**Tikkanen, M. and Aro, E.M. (2014). Integrative regulatory network of plant thylakoid energy transduction. *Trends Plant Sci.* 19, 10-17.**

Pubmed: [Author and Title](#)  
CrossRef: [Author and Title](#)  
Google Scholar: [Author Only](#) [Title Only](#) [Author and Title](#)

**Tikkanen, M., Pippo, M., Suorsa, M., Sirpio, S., Mulo, P., Vainonen, J., Vener, A., Allahverdiyeva, Y., and Aro, E.M. (2006). State transitions revisited - a buffering system for dynamic low light acclimation of Arabidopsis. *Plant Mol. Biol.* 62, 779-793.**

Pubmed: [Author and Title](#)  
CrossRef: [Author and Title](#)  
Google Scholar: [Author Only](#) [Title Only](#) [Author and Title](#)

**Tikkanen, M., Grieco, M., Kangasjarvi, S., and Aro, E. (2010). Thylakoid Protein Phosphorylation in Higher Plant Chloroplasts Optimizes Electron Transfer under Fluctuating Light. *Plant Physiol.* 152, 723-735.**

Pubmed: [Author and Title](#)  
CrossRef: [Author and Title](#)  
Google Scholar: [Author Only](#) [Title Only](#) [Author and Title](#)

**Tikkanen, M., Grieco, M., Nurmi, M., Rantala, M., Suorsa, M., and Aro, E. (2012). Regulation of the photosynthetic apparatus under fluctuating growth light. 367, 3486-3493.**

Pubmed: [Author and Title](#)  
CrossRef: [Author and Title](#)  
Google Scholar: [Author Only](#) [Title Only](#) [Author and Title](#)

**Tikkanen, M., Rantala, S., and Aro, E. (2015). Electron flow from PSII to PSI under high light is controlled by PGR5 but not by PSBS. *Front. Plant Sci.* 6, 521.**

Pubmed: [Author and Title](#)  
CrossRef: [Author and Title](#)  
Google Scholar: [Author Only](#) [Title Only](#) [Author and Title](#)

**Tiwari, A., Mamedov, F., Grieco, M., Suorsa, M., Jajoo, A., Styring, S., Tikkanen, M., and Aro, E. (2016). Photodamage of iron-sulphur clusters in photosystem I induces non-photochemical energy dissipation. *Nat. Plants* 2, 16035.**

Pubmed: [Author and Title](#)

CrossRef: [Author and Title](#)

Google Scholar: [Author Only Title Only Author and Title](#)

**Toivola, J., Nikkanen, L., Dahlström, K.M., Salminen, T.A., Lepistö, A., Vignols, F., and Rintamäki, E. (2013). Overexpression of chloroplast NADPH-dependent thioredoxin reductase in Arabidopsis enhances leaf growth and elucidates in vivo function of reductase and thioredoxin domains. *Front. Plant Sci.* 4, 389.**

Pubmed: [Author and Title](#)

CrossRef: [Author and Title](#)

Google Scholar: [Author Only Title Only Author and Title](#)

**Toth, S.Z., Schansker, G., and Strasser, R.J. (2007). A non-invasive assay of the plastoquinone pool redox state based on the OJIP-transient. *Photosynthesis Res.* 93, 193-203.**

Pubmed: [Author and Title](#)

CrossRef: [Author and Title](#)

Google Scholar: [Author Only Title Only Author and Title](#)

**Townsend, A.J., Ware, M.A., and Ruban, A.V. (2017). Dynamic interplay between photodamage and photoprotection in photosystem II. *Plant. Cell. Environ.***

Pubmed: [Author and Title](#)

CrossRef: [Author and Title](#)

Google Scholar: [Author Only Title Only Author and Title](#)

**Trotta, A., Suorsa, M., Rantala, M., Lundin, B., and Aro, E. (2016). Serine and threonine residues of plant STN7 kinase are differentially phosphorylated upon changing light conditions and specifically influence the activity and stability of the kinase. *Plant J.* 87, 484-494.**

Pubmed: [Author and Title](#)

CrossRef: [Author and Title](#)

Google Scholar: [Author Only Title Only Author and Title](#)

**Vener, A., VanKan, P., Rich, P., Ohad, I., and Andersson, B. (1997). Plastoquinol at the quinol oxidation site of reduced cytochrome b<sub>6</sub> mediates signal transduction between light and protein phosphorylation: Thylakoid protein kinase deactivation by a single-turnover flash. *Proc. Natl. Acad. Sci. U. S. A.* 94, 1585-1590.**

Pubmed: [Author and Title](#)

CrossRef: [Author and Title](#)

Google Scholar: [Author Only Title Only Author and Title](#)

**Walter, M., Chaban, C., Schutze, K., Batistic, O., Weckermann, K., Nake, C., Blazevic, D., Grefen, C., Schumacher, K., Oecking, C., Harter, K., and Kudla, J. (2004). Visualization of protein interactions in living plant cells using bimolecular fluorescence complementation. *Plant J.* 40, 428-438.**

Pubmed: [Author and Title](#)

CrossRef: [Author and Title](#)

Google Scholar: [Author Only Title Only Author and Title](#)

**Wang, C., Yamamoto, H., and Shikanai, T. (2015). Role of cyclic electron transport around photosystem I in regulating proton motive force. *Biochim. Biophys. Acta-Bioenerg.* 1847, 931-938.**

Pubmed: [Author and Title](#)

CrossRef: [Author and Title](#)

Google Scholar: [Author Only Title Only Author and Title](#)

**Wang, P., Liu, J., Liu, B., Da, Q., Feng, D., Su, J., Zhang, Y., Wang, J., and Wang, H. (2014). Ferredoxin: Thioredoxin Reductase Is Required for Proper Chloroplast Development and Is Involved in the Regulation of Plastid Gene Expression in Arabidopsis thaliana. *Mol. Plant.* 7, 1586-1590.**

Pubmed: [Author and Title](#)

CrossRef: [Author and Title](#)

Google Scholar: [Author Only Title Only Author and Title](#)

**Yamamoto, H., Peng, L., Fukao, Y., and Shikanai, T. (2011). An Src Homology 3 Domain-Like Fold Protein Forms a Ferredoxin Binding Site for the Chloroplast NADH Dehydrogenase-Like Complex in Arabidopsis. *Plant Cell* 23, 1480-1493.**

Pubmed: [Author and Title](#)

CrossRef: [Author and Title](#)

Google Scholar: [Author Only Title Only Author and Title](#)

**Yamamoto, H. and Shikanai, T. (2013). In Planta Mutagenesis of Src Homology 3 Domain-like Fold of NdhS, a Ferredoxin-binding Subunit of the Chloroplast NADH Dehydrogenase-like Complex in Arabidopsis A conserved Arg-193 plays a critical role in ferredoxin binding. *J. Biol. Chem.* 288, 36328-36337.**

Pubmed: [Author and Title](#)

CrossRef: [Author and Title](#)

Google Scholar: [Author Only Title Only Author and Title](#)

**Yamori, W., Sakata, N., Suzuki, Y., Shikanai, T., and Makino, A. (2011). Cyclic electron flow around photosystem I via chloroplast NAD(P)H dehydrogenase (NDH) complex performs a significant physiological role during photosynthesis and plant growth at low temperature in rice. *Plant J.* 68, 966-976.**

Pubmed: [Author and Title](#)  
 CrossRef: [Author and Title](#)  
 Google Scholar: [Author Only](#) [Title Only](#) [Author and Title](#)

**Yamori, W., Shikanai, T., and Makino, A. (2015). Photosystem I cyclic electron flow via chloroplast NADH dehydrogenase-like complex performs a physiological role for photosynthesis at low light (vol 5, 13908, 2015). Sci. Rep. 5, 15593.**

Pubmed: [Author and Title](#)  
 CrossRef: [Author and Title](#)  
 Google Scholar: [Author Only](#) [Title Only](#) [Author and Title](#)

**Yamori, W., Makino, A., and Shikanai, T. (2016). A physiological role of cyclic electron transport around photosystem I in sustaining photosynthesis under fluctuating light in rice. Sci. Rep. 6, 20147.**

Pubmed: [Author and Title](#)  
 CrossRef: [Author and Title](#)  
 Google Scholar: [Author Only](#) [Title Only](#) [Author and Title](#)

**Yamori, W. and Shikanai, T. (2016). Physiological Functions of Cyclic Electron Transport Around Photosystem I in Sustaining Photosynthesis and Plant Growth. Annu. Rev. Plant Biol. 67, 81-106.**

Pubmed: [Author and Title](#)  
 CrossRef: [Author and Title](#)  
 Google Scholar: [Author Only](#) [Title Only](#) [Author and Title](#)

**Yoshida, K., Hara, S., and Hisabori, T. (2015). Thioredoxin Selectivity for Thiol-Based Redox Regulation of Target Proteins in Chloroplasts. J. Biol. Chem. 290, 19540.**

Pubmed: [Author and Title](#)  
 CrossRef: [Author and Title](#)  
 Google Scholar: [Author Only](#) [Title Only](#) [Author and Title](#)

**Yoshida, K. and Hisabori, T. (2016). Two distinct redox cascades cooperatively regulate chloroplast functions and sustain plant viability. Proc. Natl. Acad. Sci. U. S. A. 113, E3967-E3976.**

Pubmed: [Author and Title](#)  
 CrossRef: [Author and Title](#)  
 Google Scholar: [Author Only](#) [Title Only](#) [Author and Title](#)

**Yoshida, K. and Hisabori, T. (2017). Distinct Electron Transfer from Ferredoxin-Thioredoxin Reductase to Multiple Thioredoxin Isoforms in Chloroplasts. Biochem. J. 474, 1347-1360, doi/10.1042/BCJ20161089.**

Pubmed: [Author and Title](#)  
 CrossRef: [Author and Title](#)  
 Google Scholar: [Author Only](#) [Title Only](#) [Author and Title](#)

**Zaffagnini, M., De Mia, M., Morisse, S., Di Giacinto, N., Marchand, C.H., Maes, A., Lemaire, S.D., and Trost, P. (2016). Protein S-nitrosylation in photosynthetic organisms: A comprehensive overview with future perspectives. Biochim. Biophys. Acta-Proteom. 1864, 952-966.**

Pubmed: [Author and Title](#)  
 CrossRef: [Author and Title](#)  
 Google Scholar: [Author Only](#) [Title Only](#) [Author and Title](#)